Universidade de Lisboa

Faculdade de Farmácia

Prevention of breast cancer brain metastases by minocycline-loaded liposomes

Daniela Alexandra Simão Vaz

Dissertação orientada pela Professora Doutora Maria Alexandra De Oliveira Silva Braga Pedreira De Brito

Mestrado em Ciências Biofarmacêuticas

2022

Universidade de Lisboa

Faculdade de Farmácia

Prevention of breast cancer brain metastases by minocycline-loaded liposomes

Daniela Alexandra Simão Vaz

Dissertação orientada pela Professora Doutora Maria Alexandra De Oliveira Silva Braga Pedreira De Brito

Mestrado em Ciências Biofarmacêuticas

2022

The present master's thesis was performed in the research group "Neurovascular Lab", from the Research Institute for Medicines (iMed.ULisboa), Faculty of Pharmacy, Universidade de Lisboa, under the supervision of Professor Doctor Maria Alexandra Brito.

This work was supported by Fundação para a Ciência e Tecnologia (FCT – PTDC/MED-ONC/29402/2017, UIDB/04138/2020 and UIDP/04138/2020).

Outputs ensuing from the present thesis

Publications in international scientific journals

Godinho-Pereira J, Vaz D, Aniceto-Romão J, Malhó R, Rocha J, Carvalheiro MC, Simões S, Gaspar MM, Brito MA. Breast cancer brain metastases: implementation and characterization of a mouse model relying on cells inoculation in the carotid artery. (in preparation)

Godinho-Pereira J, Vaz D, Aniceto-Romão J, Simões S, Gaspar MM, Corvo ML, Carvalheiro MC, Brito MA. A Trojan horse as targeting vector for minocycline-loaded liposomes: a new strategy to prevent breast cancer brain metastases formation. (in preparation)

Acknowledgements

Primeiramente gostaria de agradecer à minha orientadora, Professora Maria Alexandra Brito, por tudo o que me ensinou durante este ano. Como aluna de mestrado sei que ainda tenho muito que evoluir e por isso queria agradecer por ter puxado por mim e me ter feito ir sempre mais além do que eu achava que conseguia. Por ter sido a pessoa que mais acreditou que este trabalho podia ser concretizado com sucesso e me ter acompanhado neste primeiro desafio a sério na minha jornada na ciência.

Aos membros do Lumiar que nos acompanharam neste desafio. À Doutora Manuela Colla Carvalheiro por toda a disponibilidade, tempo e dedicação que deu a este trabalho. Nada teria sido feito sem a sua ajuda. À Doutora Sandra por ter sido uma grande contribuição durante este ano atribulado. Por todas as tardes infinitas no biotério e conversas sobre gelado para aliviar o cansaço. À professora Manuela Gaspar por ter sido fulcral neste trabalho e por toda o seu input imprescindível.

Aos membros do laboratório. Primeiramente, à Rafaela por ter me ter introduzido ao trabalho e se ter disponibilizado para me ensinar a pesar. Como um bom exemplo é sempre aquele que fica na memória, aqui fica um agradecimento por termos tornado isto uma cena para levar para a vida.

E agora sim, um mega, ginormous obrigada às "chefas" Rita e Joana. À Rita, por ter puxado por mim e me ter orientado quando eu precisava de motivação, por se ter preocupado quando não tinha de o fazer. À Joana (ou Joana grande, apesar de ela ser pequenina) por me ter feito puxar pelos meus neurónios cansados e por me ter guiado durante tempos incertos. Obrigada por toda a ajuda, disponibilidade e abertura que tiveram durante todo este ano para ler e ouvir as nossas barbaridades. Pelo sistema de senhas, post-its e "ameaças" do armário da lixivia. Palavras não são suficientes para definir toda a dedicação e paciência que tiveram, não só comigo e com as minhas 7 vozes, mas com todas nós. Depois deste ano inteiro posso dizer que estão ambas a nível 6, mas sabemos que, no que toca a esta escala, estão acima do nível 10.

À Joana Romão, por todas as viagens até ao Lumiar e por ter sido uma ajuda na loucura que foi este ano. Sempre foste uma de nós. Às meninas novas que vimos entrar e que, apesar de pouco tempo, se tornaram uma presença agradável no nosso dia-a-dia. Rute e Beatriz, por terem sido uma boa parte deste ano, espero estar a assistir à vossa tese daqui a uns meses.

À Catarina, a outra metade da melhor dupla aqui dentro. Alguém disse que nós juntas não fazemos uma e eu concordo. Não há palavras para descrever tudo o que fizeste, não só a nível de trabalho, mas também por me ouvires e me chamares à razão quando precisava. Pelas tardes a ouvir música enquanto desesperávamos e panquecas para aliviar o stress. Nunca me vou esquecer que "chorar à chuva não conta" e que nunca é tarde para ser um dinossauro extinto ou uma célula a boiar num frasco. Levo daqui que tomar banho de óculos é crucial para conseguir ver a água e que há crianças a nascer com "ogamento" (cabelo em pé) nos confins de Portugal. My fellow slytherin, Hogwarts will always be our home.

À Elsa por me ter ajudado a crescer durante ano. À Dolores pelas dores de cabeça.

To all my friends que direta ou indiretamente estiveram lá durante todo o processo. À Sara, ao Francisco, à Maria e à Carol. Obrigada por terem sofrido comigo, por me terem ouvido e por estarem lá quando mais precisava de me divertir apesar do stress.

Ao Rui, my partner in crime for life and emotional support. Por ter tido a paciência de santo e por me ter mostrado what real love feels like. Por ter estado lá quando nada corria bem e me ter ajudado a continuar. Pela compreensão e acima de tudo por todo o amor e carinho que me deste quando eu mais precisava. A vida dá voltas e nunca sabemos o dia de amanhã, mas se há uma coisa que eu sei é que tu lá vais estar para ver o fim de mais uma etapa na minha vida, mais uma de muitas que estarão por vir. 8 anos de aventuras e mais virão. Estou grata por te ter ao meu lado nesta jornada. You are home to me.

À Madalena. My emotional support. My blinking light. My person. You were always the one who believed in me when I couldn't believe in myself, I will be forever grateful for that. You made my life easier when you didn't have to, and you made things better just by being there. I know that the ties that bind us are sometimes impossible to explain. Some bonds defy distance and time and logic because some ties are simply meant to be. One thing I learned after this crazy year is that if there's an upside to free falling, it's the chance you give your friends to catch you and you caught me every time. Your hand will always be the one I'll reach for and I'm glad we survived this Great War together.

Aos meus pais por me terem permitido chegar até aqui, sem eles nada disto seria possível. Foi ano muito longo e de muita luta, mas eu sabia que, acontecesse o que acontecesse, podia sempre contar com vocês para me ajudarem a seguir em frente. Sempre foram um apoio imprescindível. Um obrigado não chega. Aos meus avós, que mesmo estando longe, estiveram sempre a torcer por mim e se preocuparam. Esta etapa concluída é de todos vocês. Ao Lucas Maria por ser uma

bolinha de pelo absurdamente fofinha. Ele contribuiu por ser muito lindo e por me fazer feliz, that is more than enough.

Cheguei até aqui e sei que daqui para a frente não vai ser fácil, mas levo comigo tudo o que aprendi durante o meu percurso este ano. Nada disto teria sido possível sem o apoio de todos aqui mencionados. Sei que cresci e evolui em muitos aspetos e posso dizer com toda a certeza que vou levar este ano para vida. Obrigada a todos por tirarem um bocadinho do vosso tempo para mim, ficarei eternamente grata.

Abstract

As the leading global cancer occurrence, breast cancer (BC) raises a major concern, especially in the disease's metastatic stage, with the brain being one of the top metastasization sites, which leaves patients with an unfortunate prognosis. During the metastatic process, BC cells (BCCs) encounter the blood-brain barrier (BBB), shielding the brain from most cytotoxic agents. Despite BBB's restricted permeability, BCCs can still reach the brain and lead to breast cancer brain metastases (BCBM) formation. Previous studies aiming to disclose a pharmacological BBB modulator able to prevent BCCs extravasation exposed minocycline hydrochloride (MH), a clinically used antibiotic, as a promising agent in preventing BBB disruption and BCCs. *In vitro* studies developed a new formulation using Ri7-217 (Ri7), an anti-transferrin receptor antibody, as a targeting vector for MH-loaded liposomes (Ri7-MH-Lip) to act upon the BBB. Hypothesizing that MH specifically delivered to the BBB could prevent BCCs' transmigration and BCBM formation, this project aimed to ascertain Ri7-MH-Lip treatment's safety in a BCBM's mouse model and establish its efficacy in preventing BCBM formation *in vivo*. To this end, we implemented and characterized a BCBM mouse model where the formulation's peripheral toxicity was evaluated through biochemical and histological analysis and shown to be insignificant. The assessment of the treatment's efficacy in preventing BCBM was based on cranial hippocampus sections' histological analysis and zonula occludens immunofluorescence evaluation 10 days after BCC's injection, where a BCBM's reduction and increment in barrier's integrity was observed. In addition, we aimed to ascertain if the treatment could, not only prevent BCCs transmigration, but also efficiently extend the life span of BCBM-bearing animals and a higher survival was observed in treated mice. Altogether, these results demonstrate the potential of Ri7-MH-Lip formulation in BBB's preservation and BCBM prevention.

Keywords: blood-brain barrier; breast cancer brain metastases; minocycline hydrochloride; liposome; *in vivo* animal model

Resumo alargado

O cancro da mama (CM) é um tumor maligno que geralmente se inicia nas células epiteliais dos ductos mamários. É atualmente a patologia maligna mais comum nas mulheres, podendo atingir 3,2 milhões de novos casos por ano até 2050. De todos os subtipos de CM, o triplo-negativo é um dos mais agressivos e propenso a desenvolver metástases encefálicas, sendo a principal causa de morte em pacientes diagnosticados com CM. Depois de estabelecidas as metástases encefálicas de CM (MECM), as opções terapêuticas são reduzidas, levando a um prognóstico devastador com apenas 20% de taxa de sobrevida ao fim de um ano. O desenvolvimento metastático é um processo altamente complexo, no qual as células do cancro da mama (CCMs) adquirem propriedades invasivas, destacando-se primeiramente do tumor primário e entrando em circulação, através da qual se irão espalhar por todo o organismo. Quando em circulação, deparam-se com a barreira hematoencefálica (BHE), uma barreira altamente seletiva, caracterizada pela expressão de complexos intercelulares que lhe conferem uma elevada impermeabilidade, de modo a limitar a entrada da maioria dos agentes citotóxicos no encéfalo. No entanto, apesar da baixa permeabilidade da BHE, as CCMs conseguem aderir às células endoteliais da microvasculatura encefálica (CEME) e comprometer as junções intercelulares e, consequentemente, a integridade da BHE, culminando na colonização do encéfalo. Deste modo, é imperativo descobrir novas estratégias preventivas que impeçam a formação de MECM. Neste sentido, estudos *in vitro* anteriores de screening de uma biblioteca de compostos, revelaram o cloridrato de minociclina (MH), um antibiótico utilizado há décadas na prática clínica, como o melhor candidato para modular as propriedades da BHE e das CCMs, prevenindo a sua transmigração para o encéfalo. Para avaliar em profundidade as propriedades da MH ao nível da BHE e na prevenção da transmigração endotelial de CCMs, foi desenvolvida uma nova nano formulação para uma entrega especifica e direcionada ao endotélio da microvasculatura encefálica, baseada num sistema de encapsulação da MH em lipossomas funcionalizados com Ri7-217 (Ri7), um anticorpo que reconhece o recetor da transferrina (TfRAb), altamente expresso nas CEME. Esta nano formulação (Ri7-MH-Lip) mostrou ser eficaz na melhoria das propriedades de BHE quando em contato com células metastáticas, bem como na prevenção da adesão de CCMs ao endotélio da BHE, validando a MH como molécula promissora no que diz respeito à prevenção da formação de MECM *in vivo*. Tendo como hipótese que a MH é capaz de impedir a transmigração de CCMs modulando as propriedades da barreira, este projeto teve como objetivo avaliar a segurança do tratamento com Ri7-MH-lip

num modelo de MECM em murganho, validar a sua eficácia na prevenção da formação de ME e determinar a sua capacidade para melhorar as propriedades da BHE *in vivo*. Sabendo que um modelo animal robusto e reprodutível com formação preferencial de ME é crucial para desenvolver novas terapias de prevenção de MECM, procedemos à implementação deste modelo em Portugal. Este novo modelo teve por base a inoculação de células 4T1 (células de CM triplo-negativo) na artéria carótida comum de murganhos Balb/c fêmea com 8-10 semanas de idade, com o objetivo de direcionar as células malignas para o encéfalo e permitir a formação preferencial de metástases encefálicas. Após a implementação do modelo, este foi caracterizado em termos do desenvolvimento de metástases encefálicas por coloração hematoxilina-eosina (HE) dos encéfalos e órgãos periféricos (pulmão, rim e fígado) a diferentes tempos (7, 10 e 14 dias) após a inoculação de células 4T1. A análise de secções do hipocampo cranial e cerebelo revelou a expansão gradual de MECM no hipocampo cranial, enquanto a sua presença foi insignificante no cerebelo. Em relação aos órgãos periféricos, apenas foram detetadas metástases nos pulmões. Com o objetivo de entender se o aumento da área tumoral ao longo do tempo resultava de uma capacidade proliferativa progressiva das CCMs, a expressão do marcador de proliferação, Ki-67, foi avaliada juntamente com o marcador epitelial, Pan-citoqueratina, aos 10 e 14 dias após inoculação de células 4T1, a fim de visualizar lesões metastáticas em cortes craniais do hipocampo. Foi observado um aumento significativo na expressão dos dois marcadores dos 10 para os 14 dias, refletindo um aumento da proliferação das células tumorais durante a progressão das metástases encefálicas e uma reaquisição de características epiteliais durante a colonização e estabelecimento das metástases. Estes resultados foram reforçados pelo padrão de expressão do marcador epitelial lectina de tomate (T-lectina) nas metástases, enfatizando a manifestação de características epiteliais pelas células tumorais ao longo do tempo. Em seguida, com o objetivo de avaliar a toxicidade da formulação desenvolvida, os órgãos periféricos (coração, pulmões, fígado e rins) de murganhos não inoculados com células tumorais foram recolhidos para análise histológica e o seu plasma foi colhido para análise de marcadores de toxicidade cardíaca, hepática e renal. Não foram observadas diferenças entre o grupo controlo e grupo tratado com a formulação, tanto na análise histológica, como na análise do plasma, sugerindo que esta não apresenta toxicidade periférica. Depois de aferir a segurança do tratamento, procedemos à avaliação da eficácia da formulação Ri7-MH-Lip com 3.5 mg/Kg de MH na prevenção da transmigração de CCMs em murganhos Balb/c fêmea de 8 a 10 semanas de idade sacrificados 10 dias após a inoculação de células 4T1 na artéria carótida comum. Através da coloração HE, foi possível observar um decréscimo significativo no número de metástases nas secções de hipocampo cranial e na região do

hipocampo em murganhos injetados com a nano formulação em comparação com o grupo controlo, embora não tenham sido observadas diferenças significativas relativamente à área de metástases entre os dois grupos. Mais ainda, analisando apenas a área do hipocampo, foi possível observar uma redução significativa no número e área de metástases nos murganhos tratados com Ri7-MH-Lip, quando comparados com o grupo controlo. Ainda com o objetivo de caracterizar o comportamento da BHE após o tratamento com Ri7-MH-Lip, a expressão de *zonula occludens* (ZO)-1, uma das mais importantes proteínas das junções de oclusão, foi avaliada por imunohistoquímica. Esta análise e quantificação revelou um aumento da expressão de ZO-1 nos vasos, sugerindo uma melhoria das propriedades da BHE após o tratamento. Por fim, este trabalho teve, ainda, como objetivo avaliar se o tratamento com Ri7-MH-Lip é capaz, não só de prevenir a transmigração de CCMs para o encéfalo, como também de prolongar o tempo de vida de murganhos portadores de MECM. Para este efeito, murganhos Balb/c foram inoculados com células 4T1 na artéria carótida comum, sendo que o grupo não tratado recebeu apenas veículo (NaCl 0,9%) e o grupo tratado recebeu o equivalente a 3.5 mg/Kg de MH por injeção. Foi monitorizada a sobrevivência ao longo do tempo e foi possível observar que os animais tratados com a formulação apresentaram um prolongamento do tempo de vida em relação ao grupo não tratado. Para validar estes resultados, procedemos ainda à análise histológica, através da coloração HE, onde foram observadas metástases totalmente desenvolvidas em cortes do hipocampo cranial no grupo não tratado, em comparação com o grupo tratado com a formulação. Em síntese, durante a realização deste trabalho foi possível implementar e caracterizar um novo modelo animal de MECM. Foi também possível demonstrar a eficácia da MH em prevenir a transmigração CCMs para o encéfalo, consequente formação de ME e preservar a integridade da BHE *in vivo*, bem como a segurança da estratégia terapêutica. Este estudo contribui, assim, para o avanço científico no desenvolvimento de novas terapias preventivas na neuroncologia, nomeadamente para MECM.

Palavras-chave: barreira hematoencefálica; metástases encefálicas do cancro da mama; cloridrato de minociclina; lipossomas; modelo animal *in vivo*

Contents

Figure index

Table index

Abbreviations

AJ - Adherens junction

ALT - Alanine aminotransferase

AMT - Adsorptive mediated transport

AST - Aspartate aminotransferase

BBB - Blood-brain barrier

BC - Breast cancer

BCBM - Breast cancer brain metastases

BCCs - Breast cancer cell

BM - brain metastases

BMEC - Brain microvascular endothelial cell

BSA - Bovine serum albumin

CD – Cluster of differentiation

Chol - Cholesterol

CK – Creatine kinase

CMT - Carrier-mediated transport

CNS - Central nervous system

CTCs – Circulating tumour cells

d - Days

DSPE-PEG - Distearoyl-glycero-phosphorylethanolamine– poly(ethyleneglycol)2000

DSPE-PEG-Maleimide - DSPE-PEG:1,2-distearoyl-sn-glycero-3-phosphoethanolamine-poly(ethyleneglycol)2000-N-maleimide

EC - Endothelial cells

EMT – epithelial-mesenchymal transition

EPC - Egg phosphadidylcholine

ER – Oestrogen receptor

FBS - Foetal bovine serum

GJ - Gap junction

HE - Hematoxylin-eosin

HEPES - N-(2-Hydroxyethyl) piperazine-N′-(2-ethanesulfonic acid)

HER2 - Human epidermal growth factor 2

HR - Hormone receptor

IHC – Immunohistochemistry

i.v. - Intravenous

JAM - Junction adhesion molecule

mAb - Monoclonal antibody

MET – mesenchyma-endothelial transition

MH - Minocycline hydrochloride

MH-Lip - Minocycline hydrochloride-loaded liposomes

MHT – Molecular trojan horse

MMP - Matrix metalloproteinase

Pancyt – Pan-cytokeratin

PBS - Phosphate-buffered saline

PEG - Polyethylene glycol

PFA – Paraformaldehyde

PR – Progesterone receptor

Ri7 - Ri7-217

Ri7-MH-Lip - minocycline-loaded liposomes

RMT - receptor-mediated transport

rpm - Rotation per minute

RPMI - Roswell Park memorial institute

TEM – Transendothelial migration

Tf - Transferrin

TfR - Transferrin receptor

TfRmAbs - Transferrin receptor monoclonal antibody

THL – Trojan horse liposomes

TJ - Tight junction

T-lectin - Tomato lectin

TN – Triple-negative

TNBC – Triple-negative breast cancer

VE – Vascular endothelial

ZO - Zonula occludens

Chapter I – Introduction

1. Breast Cancer

Breast cancer (BC) is a malignant tumour that commonly begins in the epithelial cells of the mammary ducts[1] even though it can also emerge from the milk-producing glands (lobules) of the breast[2]. In 2020, over two million new cases of BC were diagnosed worldwide, comprising the most frequent malignancy among women and being responsible for 684,996 deaths[3]. About 1.7 million new cases of BC are diagnosed every year and it is predicted that, by 2050, female BC will reach 3.2 million new cases per year. These numbers reflect the magnitude of BC incidence, its impact on society worldwide and the urgent need for preventive and treatment measures[4].

The classification of the BC subtype is a highly important determinant of patient survival and prognosis since the effectiveness of certain therapies depends on the receptor expression, along with the existence of a strong association between the subtype and metastatic pattern. Although remarkable improvements in novel therapies for primary tumour treatment increased BC patients' life quality and survival, the development of distant organ metastasis arises as a major concern[5]. As BC cells (BCCs) constitute a heterogeneous population, one of the most widely used BC classifications divides BC patients into three groups according to the receptors expressed on the BCCs surface: hormone receptor (HR)-positive, when BCCs express oestrogen and/or progesterone receptors (ER and PR, respectively); human epidermal growth factor receptor (HER) 2 -positive, where HER2 is being overexpressed; and lastly, triple-negative (TN) BC (TNBC), which is characterized by the absence of HR and HER2 overexpression. The last one enunciated is the group with the worst prognosis and lowest overall survival, as described in illustrated 1[1,6].

As cancer reaches its most advanced or metastatic stage, tumour cells have the capacity to spread and form new tumours in distant visceral organs[7]. Central nervous system (CNS) metastases from BC develop in 15-25% of patients, occurring with the highest incidences in HER2-positive and TNBC subtypes, representing the second most frequent cause of metastases development into CNS, following lung cancer[7]. Brain metastasis (BM) limit both life expectancy and quality of life, being the main cause of death in BC patients. With an annual incidence of 8.3–14.3 per 100,000 individuals, it represents a massive and devastating problem, with a survival rate of only 20% one year after diagnosis[3]. Even though metastatic cancers are responsible for about 90% of cancer mortality, most of the attention and research funds are focused on the treatment of primary tumours. Metastatic BC is considered incurable with the currently available therapies, in contrast with early diagnosed BC[7].

TNBC makes up approximately 15% of all classified BC tumours and patients having TNBC experience the worse prognosis of all subtypes, owing to higher rates of recurrence and limited therapeutic options. Moreover, TNBC is usually more aggressive and more likely to metastasize[8]. Through mammography screenings, it is possible to have early detection of BC, which improves the chances for a successful treatment and consequently a decrease in mortality. The common treatment procedure for early-stage BC involves either mastectomy or lumpectomy accompanied by adjuvant treatment[1]. The average time between primary BC diagnosis and BCBM development is the shortest for patients with TNBC[6]. Despite the therapeutic advances, the management of BM is still a significant challenge due to the absence of targeted therapies specific to this secondary tumour formation, leading to an increase in BM incidence[6]. The only available therapeutic option for TNBC is single-agent sequential chemotherapy[9]. Drug resistance is commonly observed in metastatic TNBC, therefore, effective targeted therapies are needed[8].

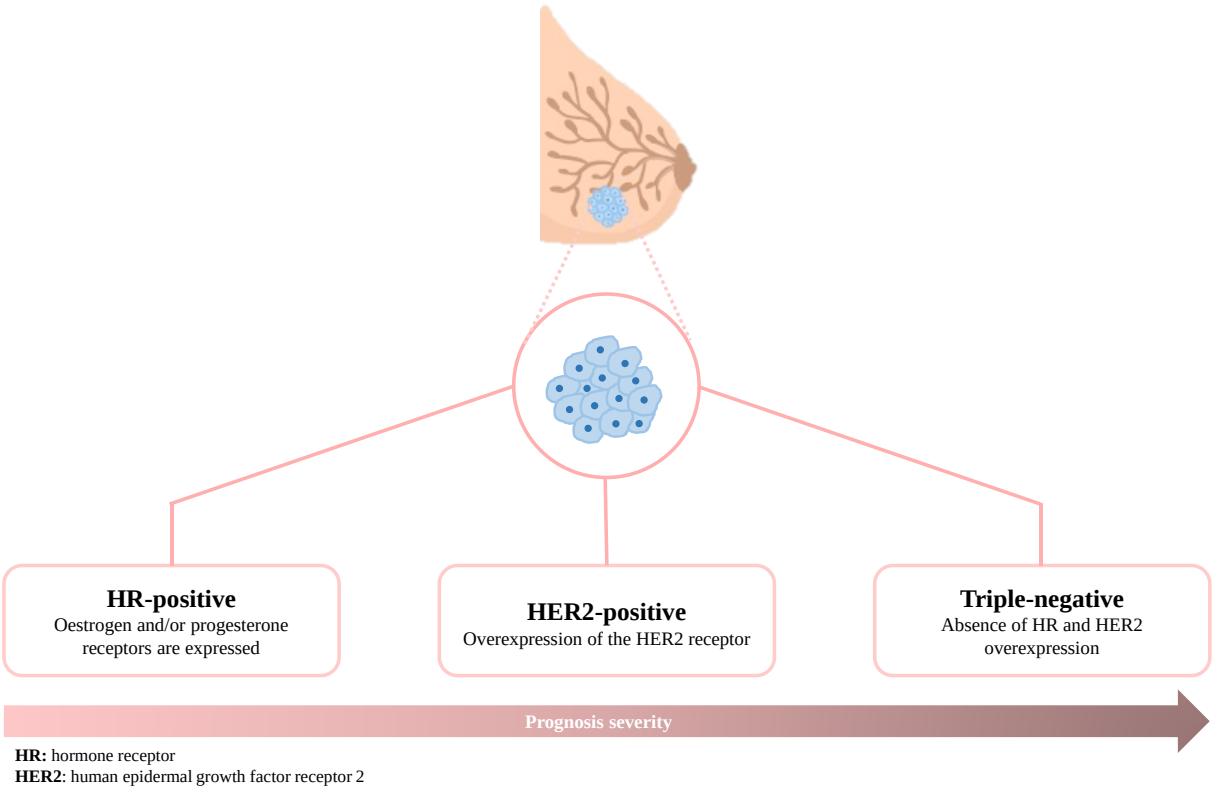

Figure 1 | Breast cancer (BC) subtypes. BC patients are commonly classified into three groups, according to the receptors expressed in BC cells (BCCs): hormone receptor (HR)-positive if oestrogen or progesterone receptors are present; human epidermal growth factor receptor (HER) 2 -positive, where HER2 is overexpressed; and triple-negative BC (TNBC), characterized by the absence of hormone receptors and HER2, presenting the worst prognosis and comprising the patients with worse predicted survival.

2. Breast cancer brain metastasis formation by metastatic cascade

Metastasis formation is a complex process comprising several steps, including: individual BCCs' invasion of the mammary tissue through the basement membrane into the surrounding tissue; dissemination from the primary tumour mass into the circulatory system (intravasation); their survival in the circulatory system; the arrest, attachment and migration of circulating tumour cells (CTCs) across brain microvascular endothelial cells (BMECs) (extravasation) and, finally the colonization of the brain parenchyma, leading to the formation of brain metastatic lesions[10], as represented in figure 2.

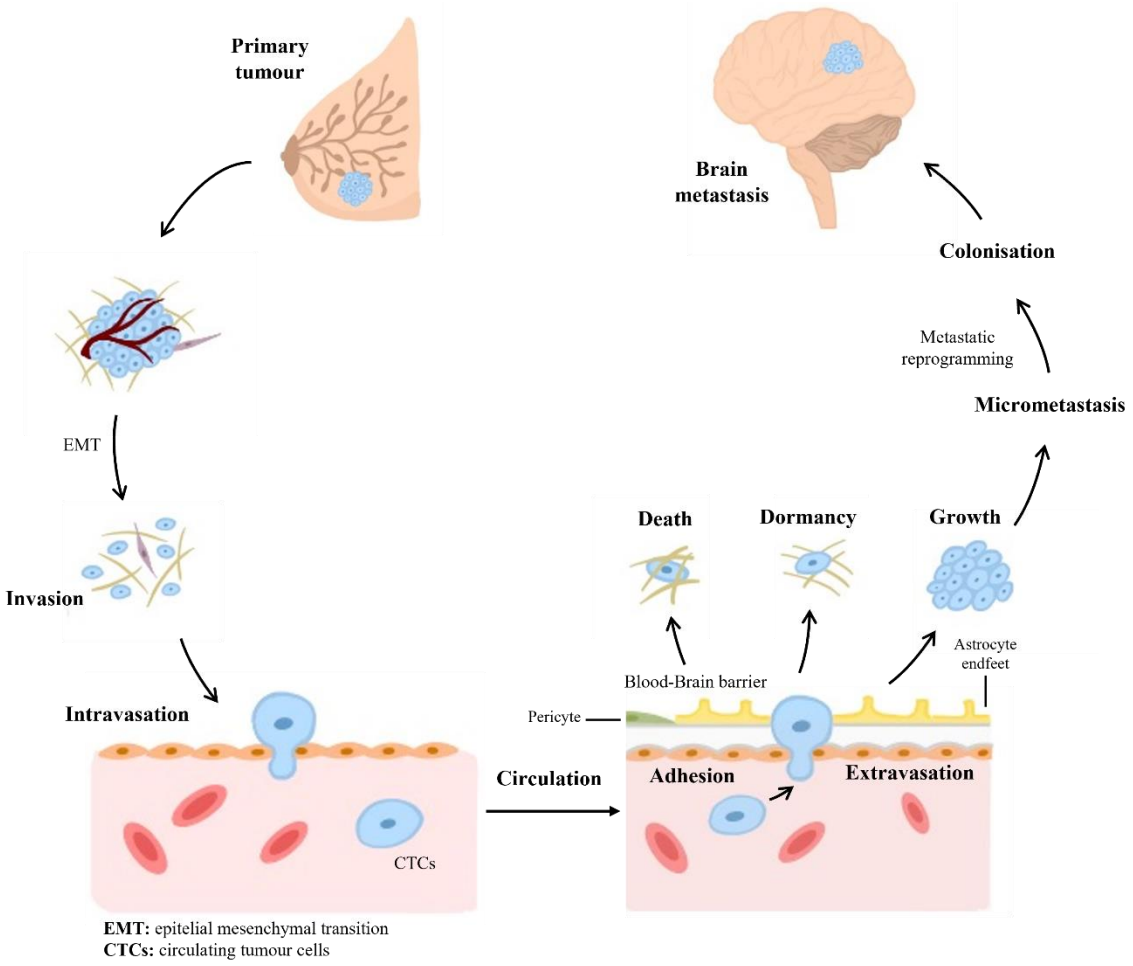

Figure 2 | Breast cancer (BC) metastatic cascade. BC brain metastasis (BCBM) formation comprises several steps, including BC cells (BCCs) invasion of the mammary tissue through the basement membrane into the surrounding tissue and dissemination from the primary tumour mass into the circulatory system (intravasation) by acquiring mesenchymal and invasive phenotype through epithelial-mesenchymal transition (EMT). Due to the bloodstream, BCCs spread throughout the circulation and interact with the blood-brain barrier (BBB), completing the metastatic cascade when the BCCs surpass the BBB and successfully colonize the brain parenchyma. In the brain, the BCCs can present 3 distinct stages: most of BCCs die; enter a state of dormancy or proliferate within this new microenvironment, forming micrometastasis. After metabolic reprogramming, tumour cells start the colonisation of brain parenchyma leading to the formation of macrometastasis. Additionally, dormant cells tend to be reawakened in a certain condition and proceed to participate in colonisation and cause tumour recurrence.

The metastatic chain begins with the separation of BCCs from the basement membrane to invade local tissues. In order to detach themselves from the tumour conglomerate, cells undergo phenotypic changes in a process called epithelial-mesenchymal transition (EMT)[6]. It is postulated that EMT occurs when cells lose their epithelial properties through the downregulation of epithelial markers, such as claudin and epithelial (E)-cadherin and gain mesenchymal traits, as the expression of mesenchymal proteins like vimentin and neuronal (N)-cadherin, leading to loss of cell polarity and adhesion ability and, consequently, acquiring invasive properties[6,11]. The replacement of E-cadherin for N-cadherin promotes the resistance to programmed cell death induced by loss of cell adhesion, or anoikis, through the modulation of apoptotic-related genes. The ability to overcome anoikis is correlated with the acquisition of the mesenchymal phenotype, allowing the survival and proliferation of BCCs without cell-cell interactions. Even though cells change their shape and motility through EMT, not all BCCs finish the process[1].

After intravasation, the survival of malignant cells in circulation is an imperative step for metastasis development. Importantly, only cancer cells with high metastatic potential survive, succeed in homing and extravasation and are able to disseminate into other organs, such as the brain[1]. Only a small fraction of BCCs can successfully survive the shear stress created by the blood flow, surveillance by immune cells and anoikis[12]. Tumour clusters have a higher probability of survival in the bloodstream and present a greater capacity to form new tumours compared to individual cells[1]. Tumour cells can express proteins with anti-apoptotic and pro-survival functions, such as the cluster of differentiation (CD)47 and other inhibitory receptors to escape natural killer (NK)cells, anti-tumour protagonists, leading to a metastasis-promoting state in which the immune escape of CTCs is favoured[12,13].

The last step of the metastatic cascade is the extravasation process, which is comprised of three sequential steps[14]. As CTCs reach the brain vasculature, their extravasation requires interaction with BMECs[1]. Firstly, CTCs are passively arrested in small capillaries, establishing an initial site of weak adhesion[12]. Endothelial (E)-selectin is a major adhesion receptor on endothelial cells (ECs) for leukocytes and has been demonstrated to support the metastatic process *in vivo*[15]. Similarly to migrating leukocytes, CTCs also express E-selectin ligands and use selectin-dependent mechanisms to adhere to BMECs followed by transmigration. In the same matter, chemokines have also been linked to transendothelial CTCs migration into the

brain parenchyma[16]. Next, a firm adhesion between BCCs and BMECs is necessary, being possible by their interaction with adhesion molecules and respective receptors, such as integrins[12,16,17]. After attachment, the previously mostly spherical cells spread on the endothelium and actively transmigrate through the blood-brain barrier (BBB) by a process called transendothelial migration (TEM)[14].

An intact physiological BBB prevents the entry of metastatic cells into the brain and the specific route by which tumour cells cross the barrier remains unclear[7,12]. TEM into the brain can occur through two pathways: transcellular route (through the ECs themselves) or paracellular route (through the intercellular junctional complexes, between ECs)[7]. These two migration pathways have been observed both in immune cells (leukocytes) and BCCs extravasation[7,18]. It is believed that, upon transcellular intravasation, the ECs' Ca2+ – calmodulin complex activates myosin light chain (MLC) kinase (MLCK) at BCCs' attachment sites, leading to local phosphorylation of MLC and actomyosin contraction. Consequently, this results in a rapid cytoskeletal and membrane remodelling, creating a transitory pore-like structure for BCCs to transverse the EC[18,19]. Although BCCs are able to transcellularly migrate through the BBB, most cancer cells, including BCCs, appear to have a preference for the paracellular route[12,18]. This interaction between BCCs and BMECs induces a redistribution and reorganization of intercellular junctions leading to BBB disruption[10,12], as illustrated in figure 3.

Once the cancer cells have exited the bloodstream and have invaded the brain parenchyma, they start to proliferate, founding a metastatic colony to establish an adequate blood supply in order to provide essential nutrients for tumour growth[12,16]. After extravasation, a considerable proportion of metastatic cells are likely to die owing to the active anti-tumour response from the organism; others become quiescent, with the risk of recurrence, and a few enter a proliferative state[12]. The colonisation of BCCs might include a sequence of events, like the reawakening from a dormancy state, vascular co-option for micrometastases formation, and metabolic reprogramming. To finish the metastatic cascade, BCCs reacquire their epithelial phenotype via mesenchymal-epithelial transition (MET) and form well-established BM. The reacquisition of epithelial phenotype by malignant cells might be the potential mechanism contributing to the establishment of macrometastases in the brain[1].

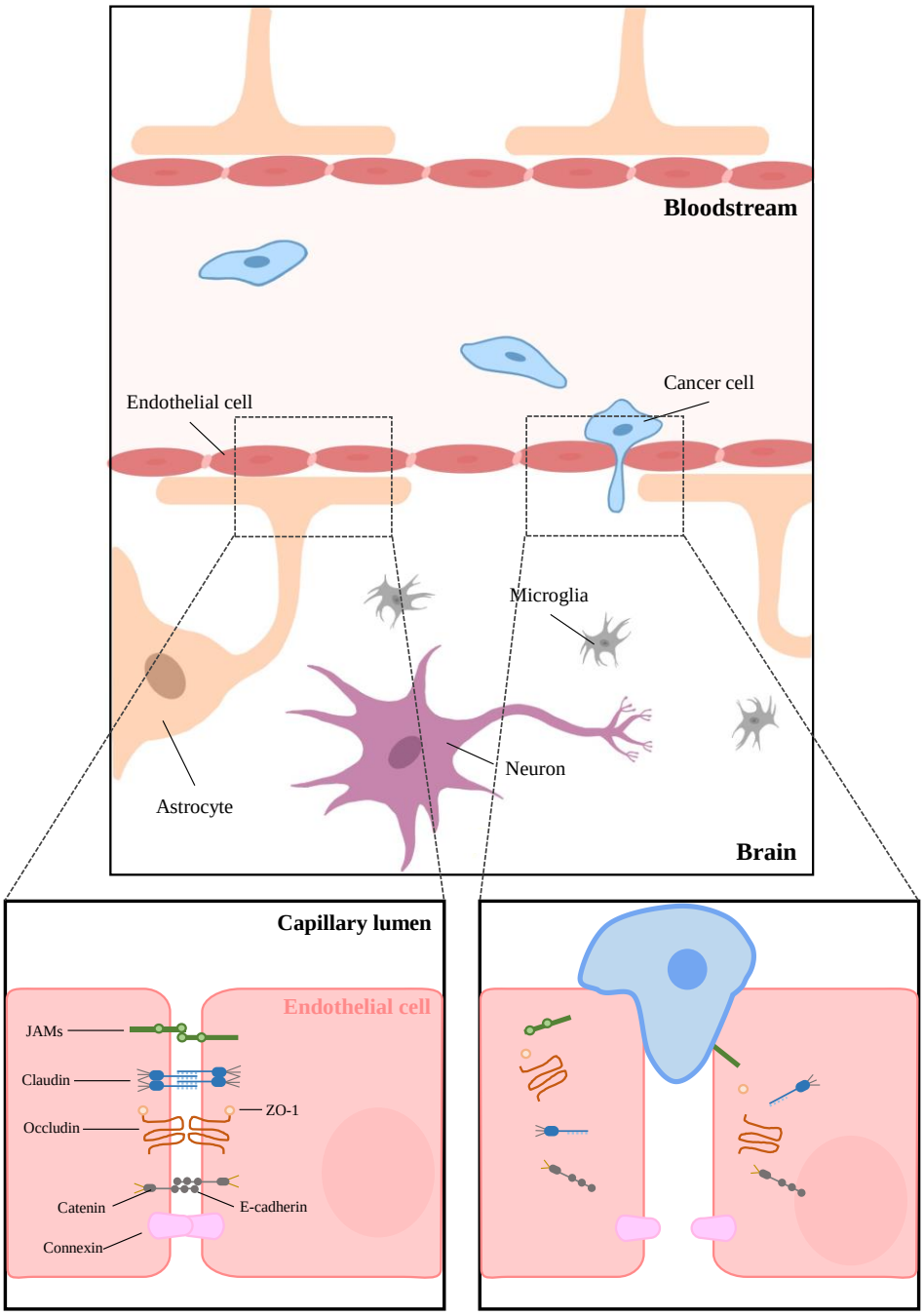

Figure 3 | Extravasation of circulating tumour cells (CTCs) across the blood-brain barrier (BBB) can lead to the disruption of junctional complexes. The interaction between CTCs and brain microvascular endothelial cells (BMECs) induces a redistribution and reorganization of intercellular junctions in order to squeeze through BMECs, leading to BBB disruption. Transmigration of CTCs into the brain parenchyma may occur through a paracellular route, passing between two endothelial cells (ECs). This process leads to a disruption of the elaborated intercellular junctional complexes between BMECs, including tight junctions (TJs) composed of occludin, claudin, zonula occludens-1 and junctional adhesion molecules (JAMs); adherens junctions (AJs) including E-cadherin and catenins; and gap junctions (GJs) mainly composed by connexins like connexin 43.

3. Blood-Brain Barrier

Located at the level of cerebral capillaries, the BBB is a complex semi-permeable, cellular-based barrier separating the brain parenchyma from systemic blood circulation, covering the entirety of the brain[20]. This highly limiting surface is meant to protect the brain from harmful substances and control the proper balance of nutrients, restricting the free movement of potentially neurotoxic plasma components, blood cells and pathogens between the systemic circulation and neuronal tissue[21,22].

As previously mentioned, the BBB is formed by a relatively thin monolayer of interlinked specialised ECs, named BMECs, supported by pericytes and astrocyte endfeet. BMECs share common features with other endothelia but differ fundamentally in their capacity to regulate the passage of molecules and cells to and from the neural parenchyma, by having a low rate of pinocytic internalization and expression of efflux pumps[23,24]. Cerebral microvasculature lining is characterized by the existence of elaborated intercellular junctional complexes between BMECs, including highly-limiting tight junctions (TJs), adherens junctions (AJs), and gap junctions (GJs)[1].

TJs play an important role in restraining paracellular transport limiting the size of the molecules able to pass freely through the BBB[23]. TJs in the CNS form approximately 4 nm pores, strictly limiting the size of molecules able to pass freely through this space along with providing the main difference between BMECs and ECs from other tissues[23,25]. These junctions are composed of three types of molecules: occludins, claudins and junctional adhesion molecules (JAMs) and intracellular proteins linked to actin cytoskeleton, such as zonula occludens (ZO)[26]. The principal claudin in BMECs is claudin-5 and it is believed that these proteins are responsible for permeability restriction[25]. As for AJs, they are mainly structural and promote tissue structural support and provide strong cellular adhesion while contributing to barrier properties[22,23]. AJs are mainly composed of vascular endothelial (VE)-cadherin and catenins[24].

Generally, only lipophilic molecules with a low molecular weight (under 400–600 Da) and of positive charge can cross the BBB[27]. Although the BBB endothelium is highly selective and limits the penetration of both solutes and cells, BCCs are still able to reach the brain parenchyma and lead to BCBM formation[1]. Accordingly, it is imperative to develop new preventive therapeutic strategies to avoid BCCs transmigration and, consequently, BCBM formation.

4. Minocycline hydrochloride as a neuroprotective agent

Minocycline hydrochloride (MH), a second-generation, semi-synthetic tetracycline with acknowledged anti-inflammatory properties and antimicrobial effects, has been clinically used for over 30 years[28,29]. MH possesses a more lipophilic profile than other tetracyclines, which increases the drug's distribution and half-life[30]. Moreover, MH shows a better pharmacokinetic profile compared to the first-generation tetracyclines when used orally, while being rapidly and completely absorbed by the gastrointestinal tract, with excellent tissue penetration and an almost complete bioavailability[28,30]. Due to its highly lipophilic properties, MH has shown superior BBB penetration in comparison with first-generation tetracyclines, promoting its accumulation in CNS and enabling its use in the treatment of several CNS diseases[28,31].

MH was reportedly involved in the attenuation of BBB disruption and the inhibition of matrix metalloproteinases (MMP), which have been implicated in BBB damage and increased permeability[32]. MH reduces brain MMP-9 in response to inflammation and an effect on MMPs can also affect the transmigration of leukocytes into the CNS, thereby reducing neuroinflammation further[33]. It was demonstrated that MH can prevent the induced breakdown of the BBB and reduce specific cytokines and MMPs participating in BBB damage[32,34]. Yang and Peers also demonstrated that a single dose of MH benefits neurovascular remodelling after a stroke[35]. The results obtained from various authors showed for the first time that MH treatment could provide neuroprotection to the BBB by decreasing the number of disrupted microvessels and preventing the disruption of the basal lamina, suggesting that it might be able to prevent BCCs penetration into the brain[32,33,36,37]. Taking this into account, previous studies performed in our laboratory showed MH's neuroprotective effects while putting to evidence its inhibitory action in BCCs migration and adhesion to the endothelium, implying its possible anti-metastatic action. This study highly supports the selection of MH as a BBB modulator, exposing its aptitude to decrease monolayer disruption as a result of BCCs exposure[38].

5. Drug delivery systems to the blood-brain barrier

The BBB represents an insurmountable barrier for most drugs, including anticancer agents, antibiotics and other macromolecular drugs. Numerous drug delivery strategies have been attempted to enhance drug properties and pharmacokinetic behaviour, such as nanotechnology, involving the use of nanocarriers, vesicles and micelles[39,40].

Nanotechnology is an essential tool when developing new systems for the efficient delivery of potential therapeutic compounds to specific sites like the BBB. Some of the known advantages of using nano-delivery systems are the reduction of adverse side effects in non-pathological tissues associated with the non-specific distribution of drugs, an increase of drug concentration at the desired site of action and, consequently, improvement of the therapeutic effectiveness by modulating drug pharmacokinetics. In addition, the suitability of nano-delivery systems also depends on the ability to recognize and establish interactions with specific ligands conjugated on the nanoparticle surface and the overexpressed molecules at the BBB (active targeting)[41]. In general, nanoparticle-assisted drug delivery increases drug bioavailability and stability while decreasing peripheral toxicity[40]. Some examples of nanocarriers for BBB drug delivery include inorganic nanoparticles, such as silica and gold, natural substrates and liposomes[20].

5.1 Liposomes as nanocarriers for BBB target drug delivery

Liposomes are the most used nanoscale drug delivery vehicle and have already seen clinical use in multiple applications, including chemotherapeutics and vaccines[20]. These nanocarriers are spherical vesicles consisting of an aqueous inner core enclosed by uni/multi-lamellar phospholipid bilayers[42]. Often composed of phospholipids, especially phosphatidylcholine, liposomes may also include other types of lipids[39]. The liposome lipid composition determines properties such as rigidity, phase transition temperature and stability, which consequently affects drug encapsulation, retention and release[20]. Generally, liposomes' components make them biologically inert and biodegradable with low inherent toxicity[39,43].

Liposomes can accommodate both hydrophobic and hydrophilic drugs in their phospholipid bilayers and aqueous core, protecting the compounds from system degradation[39,42]. Among the various carriers or drug delivery systems introduced to the present date, liposomes have several documented advantages, including increased drug loading capacity, biocompatibility and minimum toxicity[44]. There is a need for a balance between liposome stability and the eventual drug release, since the first is responsible for extending circulation time while protecting the

drug from excretion and the latter is essential for its function. For clinical translation, liposomes usually improve the safety and efficacy of the encapsulated drugs by avoiding excretion and reducing their off-target accumulation[20].

Liposomes hold an additional advantage since they may be modified in order to efficiently target a particular site of interest (e.g., BBB)[40]. Even though liposomes have lipophilic characteristics, their size prevents them from diffusing across cell membranes or even between BMECs. Instead, liposomes are able to cross the BBB via transport systems, such as adsorptive mediated transport (AMT), receptor-mediated transport (RMT), and carrier-mediated transport (CMT)[39]. Various surface modifications have been studied and developed to promote the transference of liposomal carriers across the BBB, and this is thought to have great future perspectives regarding the diagnosis and treatment of brain-located diseases[40]. Essentially, the targeting carrier systems surface needs to be decorated with adequate ligands for specific receptors overexpressed by BMECs in order to be endocytosed and have the desired effect. For this reason, drug molecules need to have a stable association with their carriers from the time of administration until they have reached the site of interest (e.g., BMECs)[44].

Recent advancements in liposomal formulations have been obtained regarding the boost of targeting efficiency of the carrier through the use of active agents or ligands to facilitate site-specific delivery. The development of "stealth" liposomes, surface functionalization of liposomes with polyethylene glycol (PEG), enhances its circulation period in the blood and suppresses the phagocytic uptake[40]. Lipids present in the outer membrane of liposomes are often conjugated with PEG to form a shield around the liposome. A dense PEG coating protects the liposome from the reticuloendothelial system, reducing its immunogenicity while improving the penetration through brain tissues[20,45]. After administration, PEG-liposomes demonstrated a great resistance in the blood compartment for extended periods while having a high affinity to accumulate predominantly within inflammation areas[46].

The functionalization of the liposomal surface with biologically active ligands has been intensely studied. These ligands include peptides, antibodies and small molecules (preferentially at the end of the PEG molecules), which specifically bind to receptors or target transporters overexpressed by BMECs[40,47]. A small fraction of the PEG molecules carries a terminal maleimide functional group to allow the conjugation of the liposome surface with thiolated targeting ligands. The targeting ligand acts as a molecular Trojan Horse (MTH) and

can be directed at an endogenous BBB receptor/transporter, such as the transferrin receptor (TfR)[48].

6. BBB receptors as molecular trojan Horses

As formerly described, in order to meet the metabolic demands of the brain, numerous receptors and transporters are present on the surface of the BBB[40]. Liposomes have three main routes by which they may deliver their cargo into the brain: AMT, CMT and RMT, as briefly mentioned above. AMT consists of the internalization of a compound through direct electrostatic interactions between BMECs' luminal surface and the cationic groups of ligands[41]. Binding to the membrane triggers the endocytosis process of the cationic compound, where it can act on its intracellular target or diffuse into the brain parenchyma and have a pharmacological effect; CMT systems are transmembrane proteins that form gates that allow substrate transport through the membrane[49]. CMT and RMT are similar systems, in which a transporter/receptor expressed by BMECs interacts with a specific ligand and triggers the internalization of the substrate-receptor complex into the intracellular compartment[23,50]. However, CMT systems generally do not undergo endocytosis to mediate transport, contrary to the RMT transport[49].

These receptors and transporters, although sharing several mechanisms, differ in the internalization of ligands. Receptors recognize a specific ligand and promote the envelopment of the whole receptor-ligand complex and its translocation towards the abluminal side of the cell, while the transporters induce a conformation change when a ligand is recognized, promoting internalization[23]. AMT is a non-specific system, whereas CMT and RMT occur via reactions with specific BMECs' proteins, such as the transferrin receptor or glutathione transporter[20]. It has been observed that, as a result of the specificity of the interaction between receptors and ligands, RMT is the most successful and commonly used strategy for liposome target delivery to the brain[40]. Liposome nanoparticles with a surface modified by transferrin, lactoferrin, glucose and PEG have proved to be effective strategies to increase the BBB permeability[43]. Liposomes targeted to TfR are the most investigated because of their abundance on the BBB[39].

6.1 Transferrin receptor

The TfR is a glycoprotein composed of two subunits and a transmembrane domain. Each subunit holds the ability to link to one transferrin (Tf) molecule, which is the protein capable of binding and carrying iron through the human body[23]. Tf is one of the most abundant plasma proteins, existing in concentrations ranging from 25 to 50 µM. Due to its high abundance in plasma, approximately only 30% of the Tf molecules are saturated with iron. Tf works as a neutralising molecule if the iron plasma concentration rapidly increases, thereby preventing the risks of accumulation of toxic non-Tf bound iron[51].

Although it is expressed in plenty of other tissues throughout the human body, TfR is overexpressed by BMECs to supply the brain with all its iron needs. Iron uptake is an extremely regulated process since abnormal amounts of iron within the CNS are associated with neurological diseases[51]. Two types of TfR isoforms have been described, namely TfR1 and TfR2[23]. Even though they show homologies in the extracellular domain, they are expressed in different patterns throughout the body. TfR2 is mainly expressed in tissues implicated in iron metabolism regulation, such as the liver and small intestines, while TfR1 is generally found on the surface of most body cells (e.g., immature erythroid cells, placental tissue, rapidly dividing cells, both normal and malignant, and hepatocytes)[51]. TfR1 is extensively expressed at the luminal membrane of BMECs to endorse the brain uptake of iron by binding to Tf saturated with iron[23].

TfR isoforms create an iron-Tf-TfR complex endocytosed by the cell. This process occurs via RMT, through a clathrin-dependant pathway. Cellular iron uptake from Tf is initiated by the binding of holo-Tf to the TfR, followed by the formation of an endosome[23,50,52,53]. When in the endosome, the lower pH will induce Tf to release its iron ions to be used by the cell. The TfR-Tf complex will then be recycled and returned to the cell surface, whereas the ligand continues its transcellular transport[23,54].

The TfR is of high interest due to its overexpression by BMECs compared to other types of ECs in the periphery, being one of the most studied and frequently exploited receptors in the field of BBB target drug delivery[20,51,55]. Iron-bound Tf has a high affinity for the TfR, therefore it has been used as a ligand for BMECs targeting[47]. Numerous authors have investigated the use of TfR-targeted liposomes as a result of TfR abundance in the BBB and were able to demonstrate an increase in brain uptake and intratumoral drug delivery, along with the enhancement of PEGylated liposomes transport to the BBB[20,39,53].

Nonetheless, the targeted liposome's application has limitations when used in *in vivo* studies[14]. The main obstacles in using TfR-targeted liposomes include the wide expression of the receptor in multiple organs besides the brain leading to a lack of tissue specificity and the competition between endogenous Tf and the targeting ligand that binds to TfR1. Due to endogenous Tf elevated levels, TfR can be saturated, reducing its targeting efficiency[20,23]. In order to overcome these limitations, several monoclonal antibodies (mAbs) and targeting peptides have been developed[20].

6.1.1 Anti-TfR monoclonal antibodies

As briefly mentioned, various MTHs can be attached to the end of the maleimide functional group present in PEGyated liposomes[56]. Trojan horse liposomes (THLs), or immunoliposomes, exploit the use of mAbs to target endogenous BBB receptors like TfR[49]. Various research studies have reported that anti-TfR mAbs (TfRmAbs) are able to bind preferentially to a TfR epitope, which is different from the Tf binding site, reducing competition between ligands and, consequently, improving receptor-binding efficiency[57]. TfRmAbs that act as MTH at the BBB are almost always species-specific[58]. The first study targeting the TfR *in vivo* was performed in the rat and reported BMECs' direct binding after systemic injection of a mouse mAb raised against the rat TfR[59]. Rat mAbs against the mouse TfR were isolated and shown to be able to act as a MTH in the mouse[53,56]. For that reason, other murine analogous variants have been produced, such as clones 8D3 and Ri7-217[51,53,56,58].

The Ri7-217 mAb is a rat IgG2a and has been used in drug delivery systems targeting the brain for a while due to its high affinity for the mouse TfR[57,60]. To determine the nanocarrying capacity of anti-TfR vectors, Paris-Robidas *et al.*[59] obtained the first direct evidence of anti-TfR Ri7-217 mAb's capacity to ferry a large number of nanoparticles into BMECs after systemic injection. Their data strongly suggests that anti-TfR mAbs can be effective BMECs targeting vectors for drug delivery. An additional study proved that Ri7-217 mAb is more selective for the brain while having no measurable uptake by the liver or kidney[60].

Using modern receptor-targeted technology by the use of muscone/Ri7-217 co-modified docetaxel liposomes for enhanced drug delivery to the brain, Kang and colleagues[57] were able to showcase that Ri7-217 has a high affinity and selectivity for the brain TfR, achieving brain targeting through TfR-mediated transcytosis. Moreover, a previous study also performed by Paris-Robidas and colleagues[61] demonstrated that anti-TfR Ri7-217 mAb injected intravenously accumulates preferentially inside BMECs, rather than just remaining bound on

their luminal side or trespassing to the brain parenchyma, along with providing compelling evidence of a wide distribution of Ri7-217 mAb throughout BMECs. This study also made clear that anti-TfR mAbs bind immensely to TfRs located on the cerebral vasculature, opening the door to new opportunities for BMECs drug targeting[59]. In addition, Bendix and colleagues[62] were able to confirm the utility of Ri7-217 mAb (in short Ri7) to obtain preferential accumulation in the BBB endothelium which is the main advantage in targeting the TfR in comparison with other BBB receptors. Along with the evident targeting ability and affinity for the brain TfR, the biodistribution and preferential accumulation in the brain endothelium support the use of anti-TfR Ri7 mAb as a vector for BMECs drug delivery[61,63]. In addition, previous *in vivo* studies were able to showcase that the majority of the Ri7-decorated nanoparticles recruited to the vessel walls were internalized by the BMECs[64]. This study deeply supports the use of this mAb as targeting vector to act upon the BBB endothelium and accumulate inside BMECs, which is the focus of our work.

To further validate these studies, a new formulation using Ri7 mAb as a targeting vector for MH-loaded liposomes (Ri7-MH-Lip) was developed in our laboratory. Through *in vitro* studies, MH's safety profile and efficacy were assessed along with the Ri7 decorated-liposomes delivery efficiency. It was demonstrated that Ri7 promotes cellular adhesion between the MH-loaded liposomes and BMECs, confirming the efficacy of using an anti-TfR mAb as a BMECs targeted delivery vector. The treatment showed no signs of toxicity and no impairments to the barrier endothelium integrity and permeability, validating the use of this nanoformulation as a preventive treatment for the transmigration of BCCs between BMECs (Rafaela Silvestre, Master thesis, Faculdade de Farmácia, Universidade de Lisboa, 2022; Joana Godinho-Pereira, PhD thesis, Faculdade de Farmácia, Universidade de Lisboa, ongoing). Therefore, it is thought that, with the delivery efficiency provided by the anti-TfR mAb decorated-liposomes and preferential accumulation at BMECs' level, MH might be able to reach BMECs and prevent BCCs penetration of the BBB into the brain by modulating the barrier properties and, consequently, prevent BCBM *in vivo*.

7. Hypothesis and Aims

As previously described, MH was disclosed as a BBB modulator, improving its properties and acting as a BBB protective agent upon exposure to BCCs. Moreover, Ri7 decorated-liposomes delivery efficiency was further confirmed through *in vitro* studies, validating the use of Ri7-MH-Lip as a preventive treatment for BCBM. In this work, we hypothesized that Ri7-MH-Lip could prevent the transendothelial migration of BCCs into the brain if specifically delivered to BMECs *in vivo*. Accordingly, this project aims to deliver MH via Ri7-functionalized liposomes to the BBB endothelium and assess Ri7-MH-Lip safety and efficacy in preventing BCCs transmigration while preserving barrier properties a the BCBM mouse model. To achieve this purpose, the following specific objectives were established:

i. Ascertain Ri7-MH-lip treatment's safety profile;
ii. Establish liposomes' efficacy in preventing BCBM;
iii. Determine the liposomes' aptitude to improve the BBB endothelium properties *in vivo*.

Chapter II – Materials and methods

1. Mouse model of BCBM

A mouse model of BCBM[10,65] was implemented and characterized in Portugal. This model relies on the inoculation of murine mammary carcinoma TN 4T1 cells, one of the most aggressive BCCs, in the common carotid artery of Balb/c mice, in order to induce preferential formation of metastases in the brain. The 4T1 cells were maintained in Roswell Park Memorial Institute (RPMI) 1640 medium supplemented with glutamine (Sigma Aldrich, St. Louis, MO, USA) and 5% heat-inactivated foetal bovine serum (FBS, Sigma Aldrich, St. Louis, MO, USA) in a 5% CO2 atmosphere at 37 ◦C. BCCs [0.2x106 cells in 150 µL of phosphate buffer saline (PBS)] were injected, under ketamine (75 mg/Kg) and medetomidine (1 mg/Kg) anaesthesia by intraperitoneal (*i.p*) injection, in the common carotid artery of 8-to-10-weeks-old Balb/c mice (Gulbenkian Institute of Science, Portugal) to direct the malignant cells to the brain and allow preferential BM formation. Mice were housed in the animal facility of the Faculty of Pharmacy.

The implementation of the mouse model counted with the contribution of team members experienced in Animal experimentation (Manuela Gaspar, Sandra Simões, Manuela Carvalheiro and João Rocha) and was mainly executed by the PhD student Joana Godinho-Pereira, all certified by the National Legal Authority (Direção Geral de Alimentação e Veterinária). Plasma, brain and/or peripheral organs were collected at day 7, 10, 14, or 18 after 4T1 cells, as depicted in Figure 4.

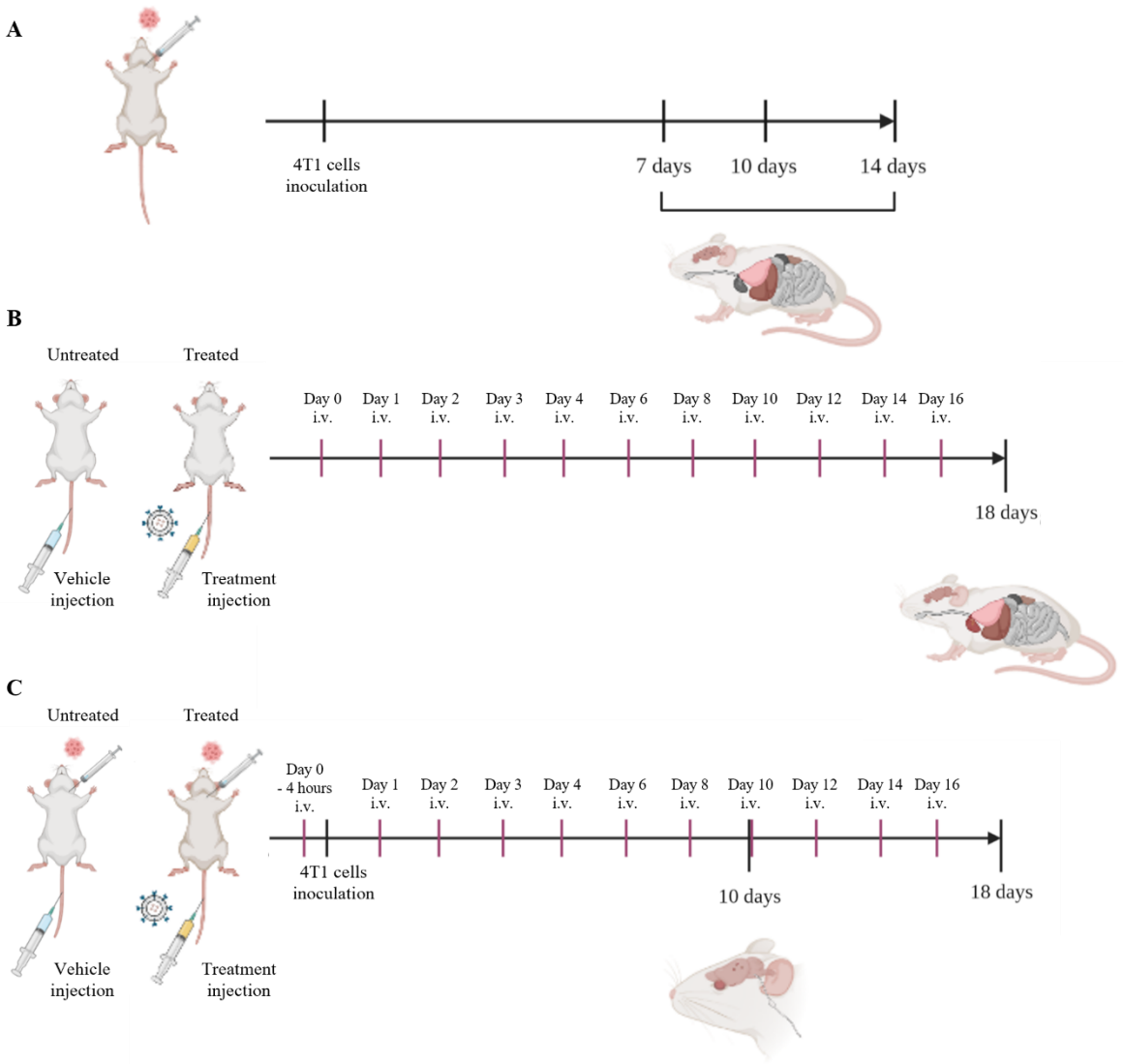

Figure 4 | Schematic representation of *in vivo* experimental design. A mouse model of breast cancer brain metastases (BCBM) was developed relying on the inoculation of murine mammary carcinoma triple negative (TN) 4T1 cells of 8-to-10-weeks-old female Balb/c mice. The sacrifice and organ harvesting were performed 7, 10, and 14 days after breast cancer cells (BCCs) inoculation (**A**). To ascertain the safety of the treatment, Balb/c mice not inoculated with 4T1 cells were injected with the Ri7-MH-Lip formulation (treated) or vehicle (untreated) in a total of 11 intravenous (i.v.) administrations. Organs and plasma collection occurred 18 days after the first liposomal injection (**B**). In order to evaluate the treatment's effectiveness in preventing BCCs transmigration, Balb/c mice inoculated with 4T1 cells were injected with Ri7-MH-Lip formulation (treated) or vehicle (untreated) and divided into two groups. A group received a total of 7 i.v. administrations and was sacrificed 10 days after 4T1 cells inoculation where brains and plasma were collected, and another group received a total of 11 i.v. administrations and was left to monitor the survival time until 18 days after BCCs injection (**C**). Created in Biorender.com.

2. Liposomes Preparation

The Ri7-MH-Lip formulation was developed in previous and still unpublished studies (Rafaela Silvestre, Master thesis, Faculdade de Farmácia, Universidade de Lisboa, 2022; Joana Godinho-Pereira, PhD thesis, Faculdade de Farmácia, Universidade de Lisboa, ongoing), in a collaboration with Doctor Manuela Colla Carvalheiro and Doctor Luísa Corvo, from the Advanced Technologies for Drug Delivery Lab, at the Research Institute for Medicines (iMed.ULisboa). The liposomes used in the present study were prepared by the PhD student Joana Godinho-Pereira, supported by Doctor Manuela Carvalheiro. Briefly, 10 mM of MH was encapsulated into liposomes (MH-Lip), composed of egg phosphatidylcholine (EPC), distearoyl-glycero-phosphorylethanolamine-poly(ethyleneglycol)$_{2000}$ (DSPE-PEG) (Lipoid GmbH, Germany) and cholesterol (Chol) (Sigma Aldrich, St. Louis, MO, USA) in a molar ratio of EPC:Chol:DSPE-PEG:DSPE-PEG at 1.85:1:0.075, respectively. MH-Lip were functionalized with Ri7 (Ri7-MH-Lip) through a post-insertion method based on the usage of micelles coupled with the Ri7 and composed by DSPC-PEG and 1,2-distearoyl-sn-glycero-3-phosphoethanolamine-poly(ethyleneglycol)2000-N-maleimide in a molar ratio of 0.06:0.015, respectively. The Ri7-MH-Lip presented a hydrodynamic diameter of 142 ± 4 nm with a polydispersity index of 0.117 ± 0.033, evidencing high homogeneity of the liposomal population. In addition, due to the PEG coating, the liposomes possessed a neutral surface charge of -2.7 mV (considered neutral from ± 4mV).

3. Plasma Collection and analysis

Blood samples were collected directly from the eye of live mice under isoflurane (IsoVet) anaesthesia into tubes containing 50 µL of the anticoagulant tri-sodium citrate [3.2% (w/v)]. The blood samples were then centrifuged for 10 minutes at 2000 rpm, at 4 ^{o}C, to remove red blood cells and buffy coat. The plasma was collected into another tube and centrifuged for 3 minutes at 13000 rpm, at 4 ^{o}C, to obtain platelet-free plasma. Biochemical parameters such as creatine kinase (CK), aspartate aminotransferase (AST), alanine aminotransferase (ALT) and urea were determined in the Biochemical Services Unit of the Faculty of Pharmacy, University of Lisbon.

4. Organ harvesting and processing

Brains and peripheral organs were collected for histological, fluorescence or immunofluorescence (IF) analysis. Anaesthetized mice were intracardially perfused with 20

mL of PBS, followed by 10 mL of 4% paraformaldehyde (PFA) in PBS to fix the tissues. The organs were harvested and postfixed overnight in 4% PFA at 4 ºC and kept in PBS also at 4 ºC.

The brains, lungs, kidneys, livers and hearts were paraffin embedded and serially cut into 4-µm-thick sections. To get different regions of the brain, coronal sections were performed following the Bregma coordinates, cerebellum, -6.12 mm; cranial hippocampus, -1.82 mm. Samples processing and sectioning was performed at the Histology and Comparative Pathology Laboratory, at the Institute of Molecular Medicine João Lobo Antunes.

4.1 Histological analysis

To depict metastases, histological analysis of brain and peripheral organs was performed. To this end, hematoxylin-eosin (HE) staining of the sections was performed at the Histology and Comparative Pathology Laboratory.

4.2 Fluorescence and Immunofluorescence

Brain sections were processed for fluorescence analysis of epithelial marker tomato lectin (T-lectin) or analysis of the target proteins. Sections were deparaffinized in xylene (20 minutes) and rehydrated through successive immersion in 100% ethanol (20 minutes), 96% ethanol (10 minutes), 70% ethanol (10 minutes), and finally tap water (10 minutes). Heat-mediated antigen retrieval was performed with 10 mM citrate buffer pH 6.0 for 15 minutes in the microwave. A permeabilization step was performed with 0.5% Triton X-100 (VWR International, Radnor, PA, USA) for 15 minutes, and tissue sections were blocked with 3% bovine serum albumin (BSA, Sigma Aldrich, St. Louis, MO, USA) containing 0.5% Triton X-100, for 60 minutes. To visualize BCCs with an epithelial phenotype, sections were incubated with fluorescein-labelled T-lectin (1:500, Vector Laboratories #FL-1171). Analysis of Ki-67, pan cytokeratin (pancyt) and ZO-1 expression was performed by IF analysis using the antibodies summarized in Table 1, diluted in blocking solution. Incubation was firstly performed with the primary antibodies overnight at 4 ºC and secondly with the respective fluorescent-labelled secondary antibodies, which took place in the dark for 60 minutes at room temperature. Between the several steps following the antigen retrieval treatment, the sections were washed with PBS. Nuclei were labelled with Hoechst 33342 dye (1:1000, Thermo Scientific, #62249) for 10 minutes, followed by mounting solution (SlowFade® Diamond Antifade Mountant, Thermo Fisher Scientific, #S36963).

Table 1 | Summary of the antibodies used in immunofluorescence analysis.

Marker	Primary Antibody	Secondary Antibody
Ki-67	Ki-67 (1:100) Thermo Fisher Scientific #PA5-19462, Rabbit Pc	Alexa Fluor® 555 (1:500) Thermo Fisher Scientific, #A-21428, Goat anti-Rabbit
Pan cytokeratin	Pan Cytokeratin (1:100) Thermo Fisher Scientific #MA5-12231, Mouse Mc	Alexa Fluor® 488 (1:500) ThermoFisher Scientific, #A-11001 Goat anti-mouse
ZO-1	ZO-1 (1:50) Thermo Fisher Scientific, #40-2200, Rabbit Mc	Alexa Fluor® 555 (1:500) Thermo Fisher Scientific, #A-21428, Goat anti-Rabbit

ZO-1, zonula occludens-1.

5. Image Acquisition

Images of HE staining were obtained using an Olympus BX51 Microscope equipped with a DP50 digital camera and Olympus Plan Apo 10x and 20x objectives. Fluorescence images were acquired using a fluorescence microscope (Olympus, Tokyo, Japan, BX60) with a mercury fluorescence illuminator and a Nomarski/DIC Prism for Transmitted Light at the Faculty of Sciences, University of Lisbon Microscopy Facility, a node of the Portuguese Platform for BioImaging (reference PPBI-POCI-01-0145-FEDER-022122), under collaboration with Professor Rui Malhó.

6. Data Analysis

For the analysis of metastases area in the cranial hippocampus and cerebellum sections along with peripheral organs, the total tumour area was determined by delimitation of each metastasis in cranial hippocampus sections at each timepoint using ImageJ 1.29x software (National Institutes of Health, USA) and the results were expressed in tumour area (mm^2). IF analysis relied on the examination of cranial hippocampus sections, a prone region for metastasis development[65]. In this sense, ten fields of the cranial hippocampus of each animal were acquired under the same conditions and analysed using the ImageJ 1.29x software and Icy software (Institute Pasteur and France BioImaging, Paris, France).

7. Statistical Analysis

Results were analysed using GraphPad Prism® 6.0 (GraphPad Software, USA) and are expressed as means ± SEM. Data normality was tested with D'Agostino Pearson and Shapiro-Wilk test. When normality was verified, the significance of data difference amongst treatment and controls was tested with the Student's *t*-test and the analysis of variance with a one-way ANOVA test amongst different timepoints and organs. When no normality between data was

observed, the significance of differences was evaluated with Mann-Whitney and Kolmogorov-Smirnov (nonparametric) tests amongst different timepoints and organs. Differences were considered statistically significant when $p<0.05$.

Chapter III - Results

1. Animal model implementation and characterization

A mouse model of BCBM relying on the inoculation of murine mammary carcinoma TN 4T1 cells in the common carotid artery of Balb/c mice was previously established at the "Neurovascular Unit Research" group, from the Institute of Biophysics of the Biological Research Centre of the Hungarian Academy of Sciences, Szeged, Hungary, by Doctor Istvan Krizbai and Doctor Imola Wilhelm. The mouse model consisted of the inoculation of $1x10^6$ 4T1 cells (TN BCCs) in 200µL of Ringer-HEPES in the common carotid artery of 8-to-10-weeks-old female mice to direct the malignant cells to the brain and allow preferential BM formation. This model was characterized by a high number of BM in coronal sections of the cranial hippocampus, with a lower and similar pattern of metastasization in the lungs and cerebellum[65].

Our aim of testing the efficacy and safety of Ri7-MH-Lip prompted us to establish such a BCBM model in our facilities in Lisbon. In our hands, the injection of the referred amount of 4T1 cells led to an extensive rate of death by embolism. In addition, the animals presented a higher survival rate when the total cellular volume was not injected, suggesting that a change in the experimental procedure was imperative. As a result, we proceeded to reduce cell concentration and volume to $0.2x10^6$ 4T1 cells in 150 µL of PBS, in line with other reports for TNBC cells[66].

1.1 Well-established metastases are detected in the brain from 7-days onwards

Metastases development and evolution were characterized by inspecting cranial hippocampal and cerebellum sections (the most and least affected sections in the original model, respectively) at different timepoints [7, 10 and 14 days (d)] after inoculation of TN BCCs in 8-to-10-weeks-old female Balb/c mice (Figure 5). Observation of HE-stained sections revealed well-established metastases observed from 7d onwards and that the injection of 4T1 cells leads to a time-dependent formation of metastases in the cranial hippocampus section (Figure 5A), whereas their presence was insignificant in the cerebellum (Figure 5B). The analysis of metastases number (Figure 5C) and area (Figure 5D) revealed a significant increment throughout time in cranial hippocampus sections. Regarding the hippocampus, it was possible to observe a significant increase in metastases number (Figure 5E) and a substantial enlargement in metastases area (Figure 5F) throughout time. The semi-quantitative analysis of tumour number (Figure 5G) and area (Figure 5H) in the cerebellum sections revealed no significant presence of BCBM.

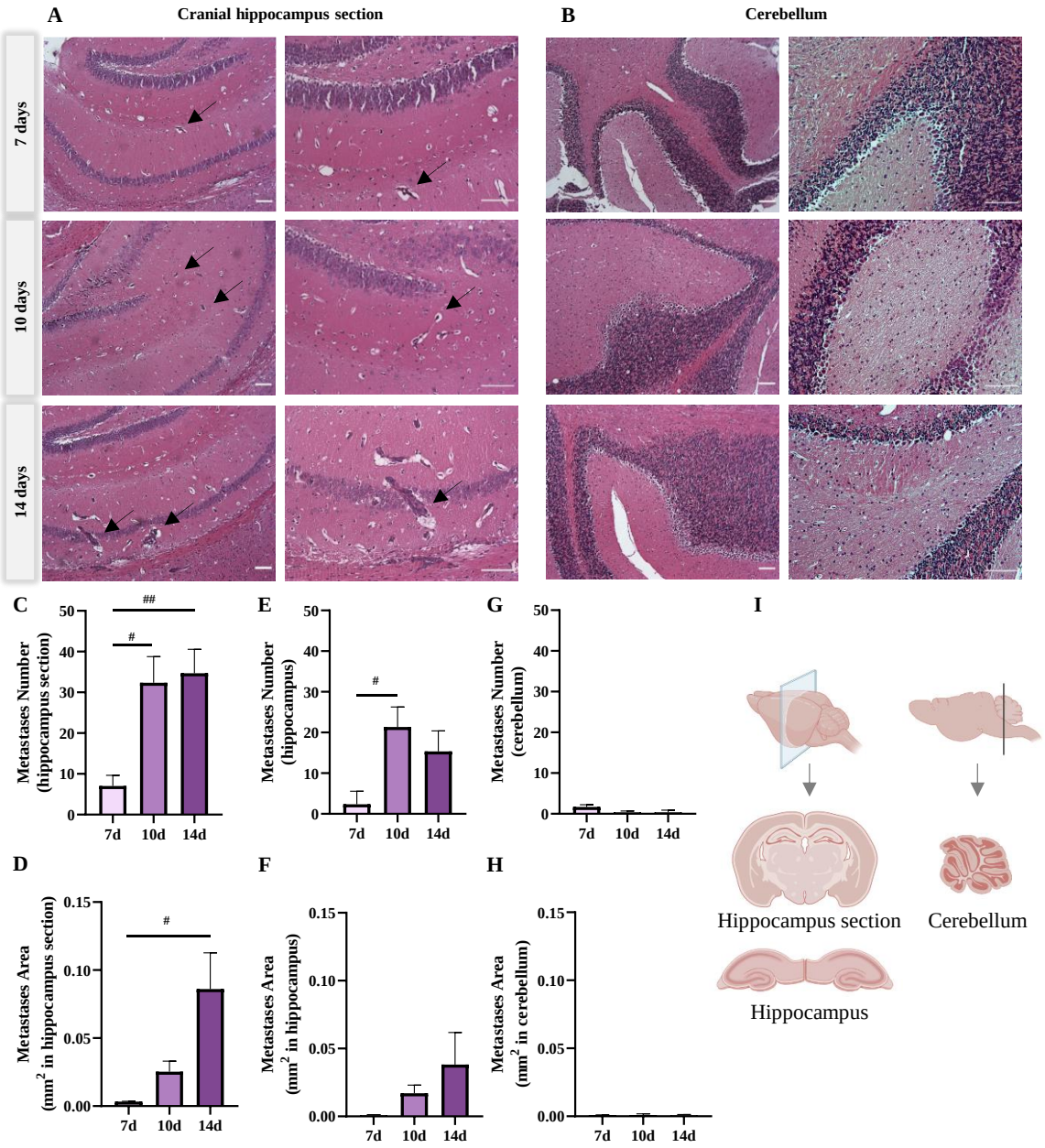

Figure 5 | Profile of breast cancer brain metastases (BCBM) in a mouse model. Cranial hippocampal and cerebellum sections were analysed, and metastases number and area were quantified at different timepoints [7, 10 and 14 days (d)] after inoculation of triple-negative (TN) breast cancer cells (BCCs) in 8-to-10-weeks-old female Balb/c mice. The pattern of BCBM formation was assessed by hematoxylin-eosin (HE) staining and well-established metastases from 7d onwards were detected. The analysis of the cranial hippocampus section revealed a time-dependent formation of metastases (black arrows) (**A**), while no metastases were detected in the cerebellum (**B**). Scale bar: 100 μm. Quantification of metastases number (**C**) and area (**D**) in cranial hippocampus sections disclosed an increment throughout time. A similar BCBM pattern in number (**E**) and area (**F**) was seen in the hippocampus region. The pattern of BCBM formation in the cerebellum and the semi-quantitative analysis of tumour number (**G**) and area (**H**) revealed no significant presence of metastases. Schematic representation of the analysed regions. Created in Biorender.com (**I**). The results are expressed as mean ± SEM (n = 3 for each timepoint). A one-way ANOVA was used to assay the significant changes in parameters between indicated timepoints. Statistical significances are denoted as # $p<0.05$ and ## $p<0.01$ between timepoints.

1.2 Peripheral breast cancer metastases were only detected in the lungs

Regarding the peripheral organs, mice's lungs, kidneys and livers were harvested at different timepoints (7, 10 and 14 d) after inoculation of 4T1 cells in 8-to-10-weeks-old female Balb/c mice. The presence of metastases was evaluated based on HE staining (Figure 6). Metastases were observed from 7d onwards in the mice's lungs (Figure 6A), whereas no metastases were detected in the other peripheral organs (liver and kidneys, Figure 6B-C). Metastases area was quantified and normalized for the analysed organ tissue, showing an increase in tumour area throughout time (Figure 6D).

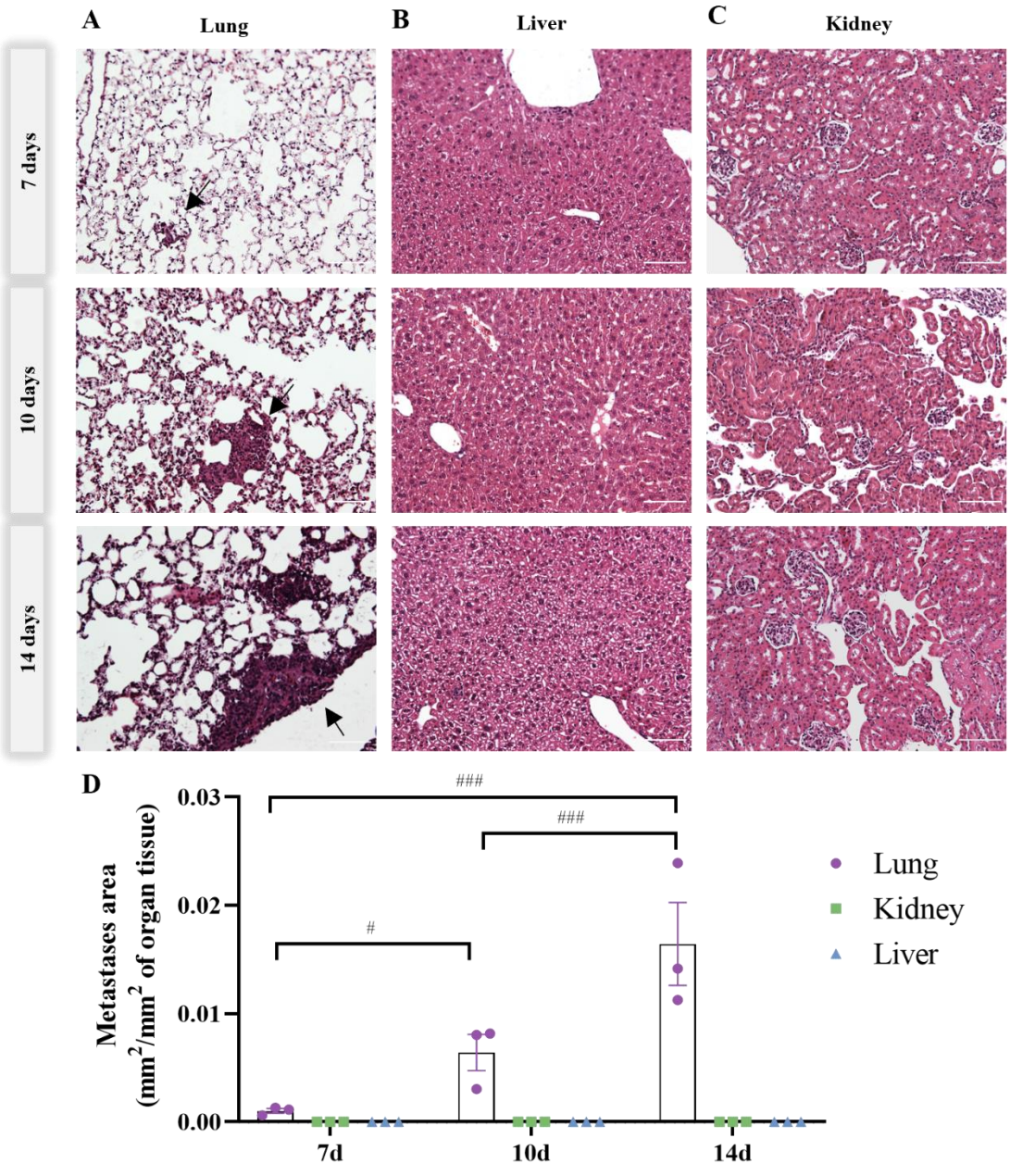

Figure 6 | Profile of breast cancer brain metastases (BCBM) in peripheral organs. Triple-negative (TN) breast cancer cells (BCCs) were injected in the common carotid artery of 8-to-10-weeks-old female Balb/c mice. The presence of metastases was assessed by hematoxylin-eosin (HE) staining in lungs (**A**), livers (**B**) and kidneys (**C**) at different timepoints [7, 10 and 14 days (d)]. Scale bar: 100 μm. Fully developed metastases were observed from 7d onwards in the mice's lungs (black arrows), whereas no metastases were detected in the other peripheral organs. Metastases area was quantified and normalized for the organ tissue (**D**). The results are expressed as mean ± SEM (n=3 for each timepoint). A one-way ANOVA was used to determine significant changes in parameters between the different timepoints and studied organs.

1.3 BCCs acquire a proliferative and epithelial phenotype during brain metastasis formation

Aiming to understand if an increasing metastatic area over time resulted from a progressive proliferative capacity of BCCs, the expression of the proliferation marker, Ki-67, was assessed. In parallel, the epithelial marker expressed by malignant cells, Pan-cytokeratin (Pancyt), was also inspected, in order to visualize metastatic lesions in cranial hippocampal sections 10 and 14 days after BCCs injection (Figure 7A). A proliferative phenotype (Ki-67-positive BCCs in BM), along with a substantial Pancyt expression 10 days after the inoculation of 4T1 cells, was observed. Notably, the immunoreactivity of Ki-67 significantly increased from 10 to 14 days (Figure 7B), reflecting metastatic cells' proliferation during BCBM progression, in accord with the enlargement of metastases area from 10 to 14 days (Figure 5D). Furthermore, the mean intensity of Pancyt significantly increased with the metastatic stage (Figure 7C), suggesting that tumour cells progressively regain epithelial features during BCBM's establishment and colonization. This is reinforced by the expression of the epithelial marker T-lectin in BCBM (Figure 7D), which emphasizes the manifestation of epithelial characteristics by tumour cells throughout time. The overall results illustrate an upregulation of epithelial markers in BCCs as metastases development progresses, suggesting the occurrence of MET.

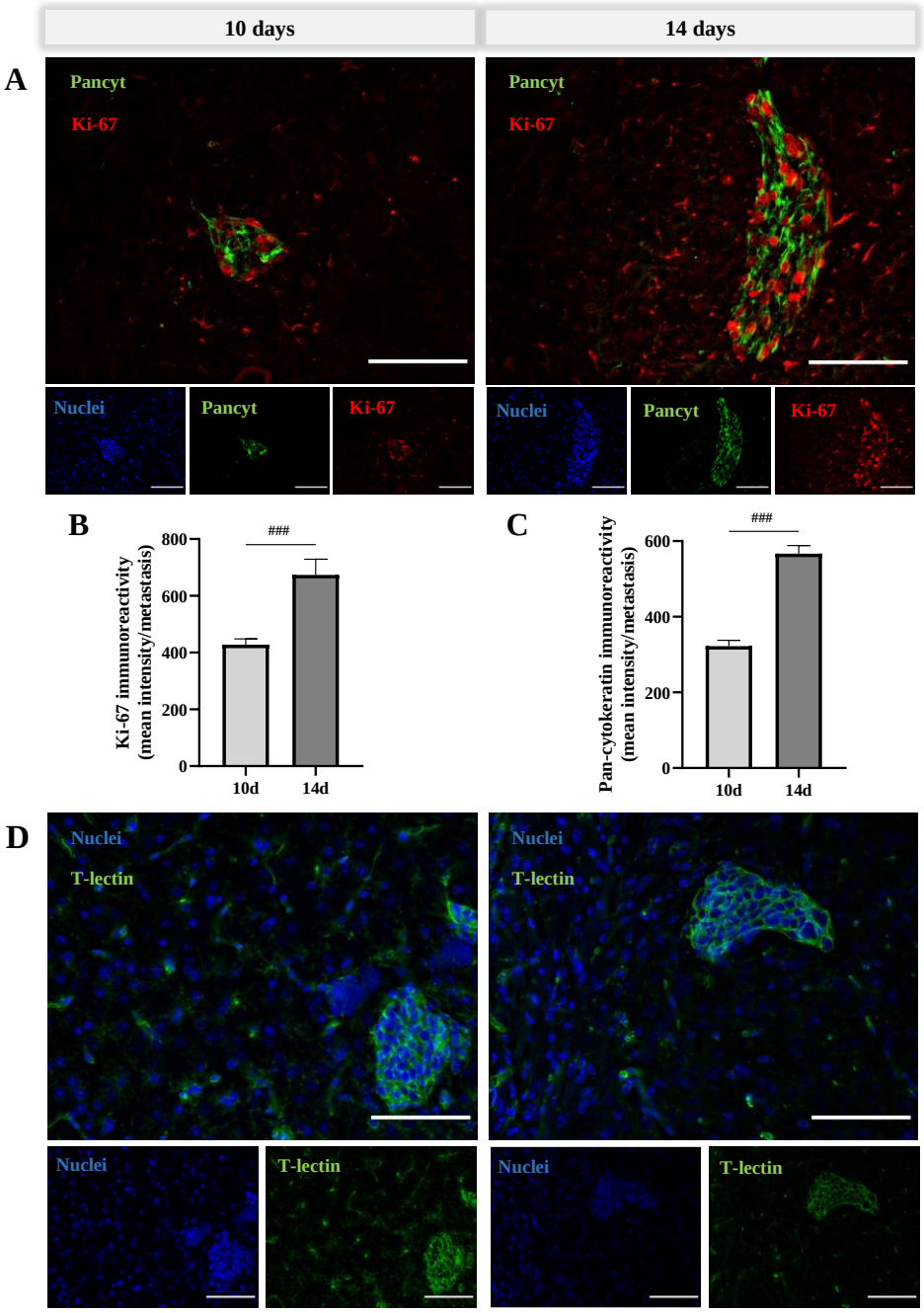

Figure 7 | Characterization of the breast cancer brain metastasis (BCBM) mouse model by fluorescence/immunofluorescence analysis. Triple-negative (TN) breast cancer cells (BCCs) were injected in the common carotid artery of 8-to-10-weeks-old female Balb/c mice and fluorescence/immunofluorescence analysis was performed in cranial hippocampal sections 10 and 14 days (d) after. Double labelling with a proliferation and an epithelial marker, Ki-67 (red) and Pan-cytokeratin (Pancyt, green), respectively, showed Ki-67-positive and Pancyt-positive metastases (**A**). Scale bar: 100 µm. Semi-quantitative analysis of Ki-67 and Pancyt showcased an increase in mean intensity in a time-dependent manner (**B-C**). The epithelial marker tomato lectin (T-lectin, green) fluorescence revealed T-lectin-positive brain metastases (**D**). Hoechst 33342 was used as counterstaining for nuclei (blue). Scale bar: 100 µm. Data is given as mean ± SEM (n = 3, 10 fields/condition). A Kolmogorov-Smirnov test was used to evaluate the significant differences between different timepoints. Statistical significances are denoted as ### $p < 0.001$ between timepoints.

2. Ri7-MH-Lip treatment presents no toxic effects

To ascertain the safety of the Ri7-MH-loaded liposomes (Figure 8), mice that did not receive any tumour cells were divided into two groups: a treated group (n = 6), where the mice were intravenously injected with Ri7-MH-loaded liposomes equivalent to 3.5 mg/Kg of MH per injection, in a total of 11 administrations along 18 days and an untreated group (n = 5), where only the vehicle (NaCl 0.9%) was injected. During the study period, animals of both groups were regularly monitored for clinical symptoms of toxicity and the body weight was measured upon each drug or vehicle administration and at the end of the experiment. The body weight was recorded at the beginning of the experiment (day 0) immediately before administration of the first dose and at the end of the experiment (day 18). Weight measurement showcased no significant weight loss between the control and treated groups since day 0 (Figure 8A).

At day 18 after the liposomal injections, blood samples were collected for biochemical analysis of toxicity indicators in plasma, following which the animals were sacrificed and peripheral organs (heart, lung, liver, and kidney) along with the brain were harvested and subjected to histological analysis to detect eventual signs parenchymal alterations. No significant differences between the two groups were observed in the plasma analysis of CK, AST, ALT, as well as urea, indicators of heart, liver and kidney toxicity, respectively (Figure 8B-E). In addition, histological analysis of brain and peripheral organs (Figure 8F) revealed no signs of deterioration, suggesting that the treatment did not elicit peripheral toxicity.

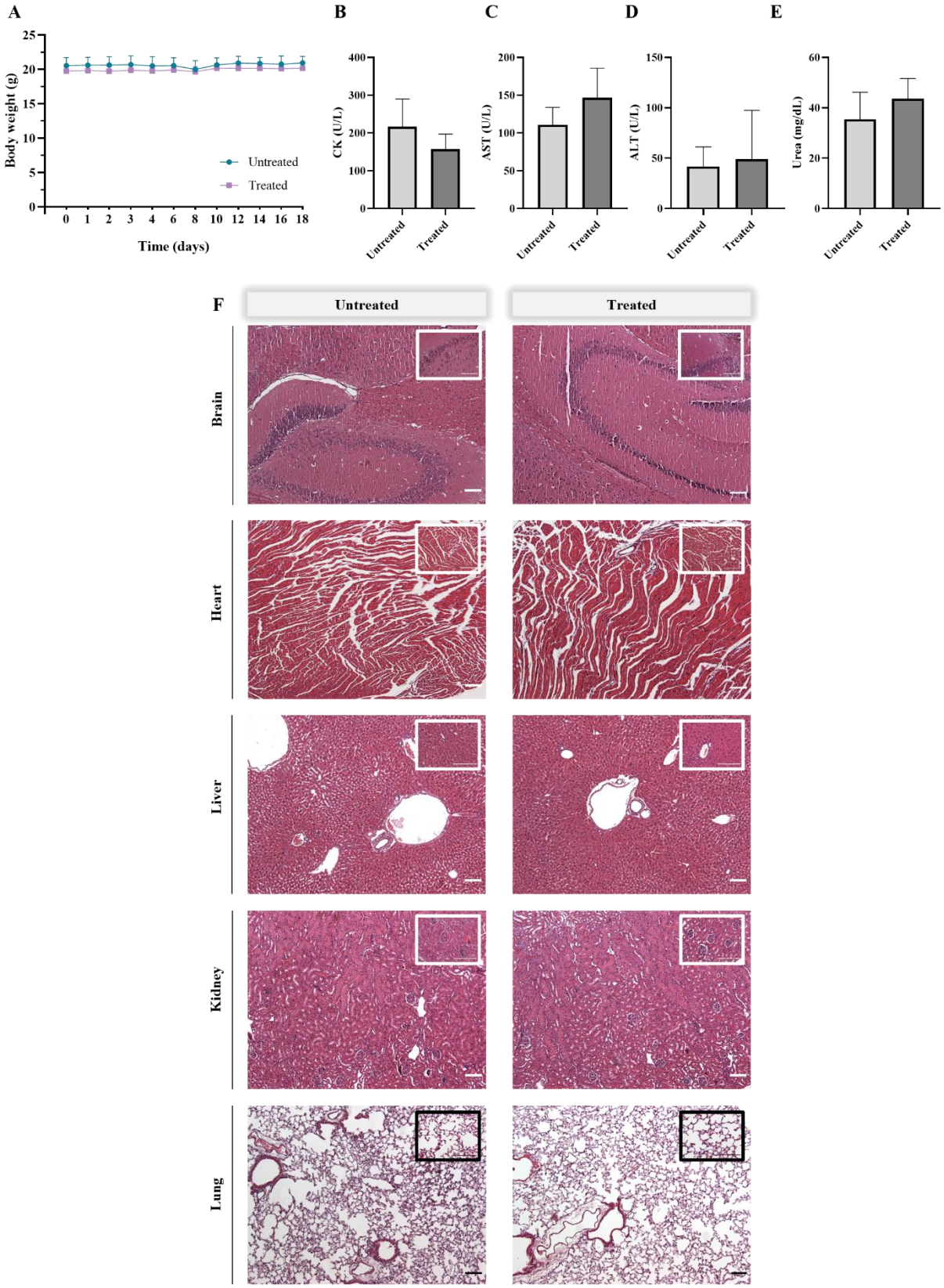
A
Body weight (g)
Time (days)
Untreated
Treated
B
CK (U/L)
C
AST (U/L)
D
ALT (U/L)
E
Urea (mg/dL)
F
Untreated
Treated
Brain
Heart
Liver
Kidney
Lung

Figure 8 | Ri7-MH-Lip treatment's safety profile in mice. To ascertain the safety of the liposomes, 8-to-10-weeks-old female Balb/c mice were injected with Ri7-MH-loaded liposomes (treated) or vehicle (untreated). The body weight of both groups was monitored along treatment and no significant weight loss was observed (**A**). Plasma samples were inspected for cardiac, hepatic and renal toxicity indicators like creatine kinase (CK) (**B**), aspartate aminotransferase (AST) (**C**) and alanine aminotransferase (ALT) (**D**), as well as urea (**E**), respectively, with no significant differences observed. Brain and peripheral organs (hearts, livers, kidneys and lungs) were harvested and subjected to histological analysis by hematoxylin-eosin staining, which revealed no signs of toxicity (**F**). Scale bar: 100 μm. The results are expressed as mean ± SEM (n = 5-6). Statistical significances were evaluated with the Mann-Whitney test.

3. MH's effect on BCCs extravasation into the brain

3.1 MH treatment reduces metastases number and area in the cranial hippocampus

The characterization of metastases' progression at different timepoints after TN BCCs' inoculation in the common carotid artery revealed that the original model's 7d timepoint shared a similar metastatic pattern with our 10d timepoint and that the majority of metastases were found in the cranial hippocampus section. These results lead us to choose the 10d timepoint and the cranial hippocampus for further evaluations.

To assess Ri7-MH-Lip treatment's effectiveness in preventing BCCs' transmigration in the established BCBM mouse model, Balb/c mice were inoculated with BCCs. A control (untreated) group (n = 8) received a saline solution (NaCl 0.9%) by intravenous injection in the tail, while a treated group (n = 7) received liposomal injections containing equivalently 3.5 mg/Kg of MH per injection, in a total of 7 administrations along 8 days. The animals were sacrificed 10 days after BCCs' injection and coronal sections of the cranial hippocampus (depicted in Figure 5I) were analysed (HE staining) for the presence and extension of metastases. A reduction of metastases was observed in the Ri7-MH-Lip-treated group, when compared to the untreated one (Figure 9A). Furthermore, quantification of metastases extension revealed a significant decrease in the number of lesions in treated mice (Figure 9B), even though no significant difference was observed regarding the area of metastases between the two groups (Figure 9C). Focusing our analysis specially in the hippocampus area (depicted in Figure 4I), a significant reduction in metastases number (Figure 9D) and area (Figure 9E) in the MH-treated mice, when compared to the control mice, was observed.

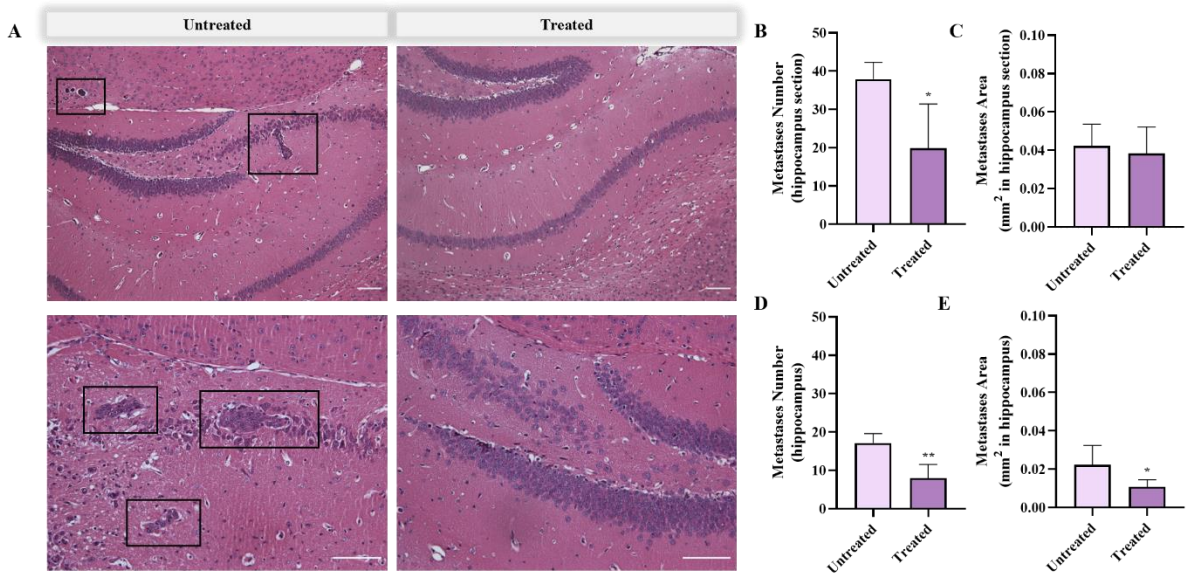

Figure 9 | Effect of RI7-MH-Lip on the prevention of breast cancer brain metastasis (BCBM) development. Triple-negative (TN) breast cancer cells (BCCs) were injected in the common carotid artery of 8-to-10-weeks-old female Balb/c mice. The pattern of BCBM colonization assessed by hematoxylin-eosin (HE) staining revealed fully developed metastases (black squares) in cranial hippocampus sections at 10 days post-tumour cells injection in the control group (untreated) by comparison to the group treated with 3.5 mg/Kg of RI7-MH-Lip (treated) which revealed almost none (**A**). Scale bar: 100 μm. The observations were supported by the quantification of the metastases number (**B**) and area (**C**) in the cranial hippocampus section where it was disclosed a significant decrease in BCBM number and a similar tumour area, when comparing with the untreated group. In the hippocampus region, a significant reduction was found in tumour number (**D**) and area (**E**). The results are expressed as mean ± SEM (n=7-8). Statistical significances were evaluated with the Kruskal-Wallis test for number and area. Statistical significances are denoted as * $p<0.05$ and ** $p<0.01$ vs untreated.

3.2 BBB's integrity is improved by 10 days after Ri7-MH-Lip Treatment

We next aimed to understand whether Ri7-MH-Lip were able to preserve BBB's integrity upon exposure to BCCs. To this end, expression of ZO-1 (Figure 10A), a TJ protein essential to barrier properties' maintenance and a relevant marker of barrier integrity[24,26] was assessed in mice inoculated with BBCs and treated with the liposomes. An in-depth quantitative analysis of ZO-1 expression at the vessels' level revealed an increase in fluorescence intensity in the animals injected with Ri7-MH-loaded liposomes (Figure 10B), suggesting an improvement in barrier integrity and a reduction in permeability when compared to the control group.

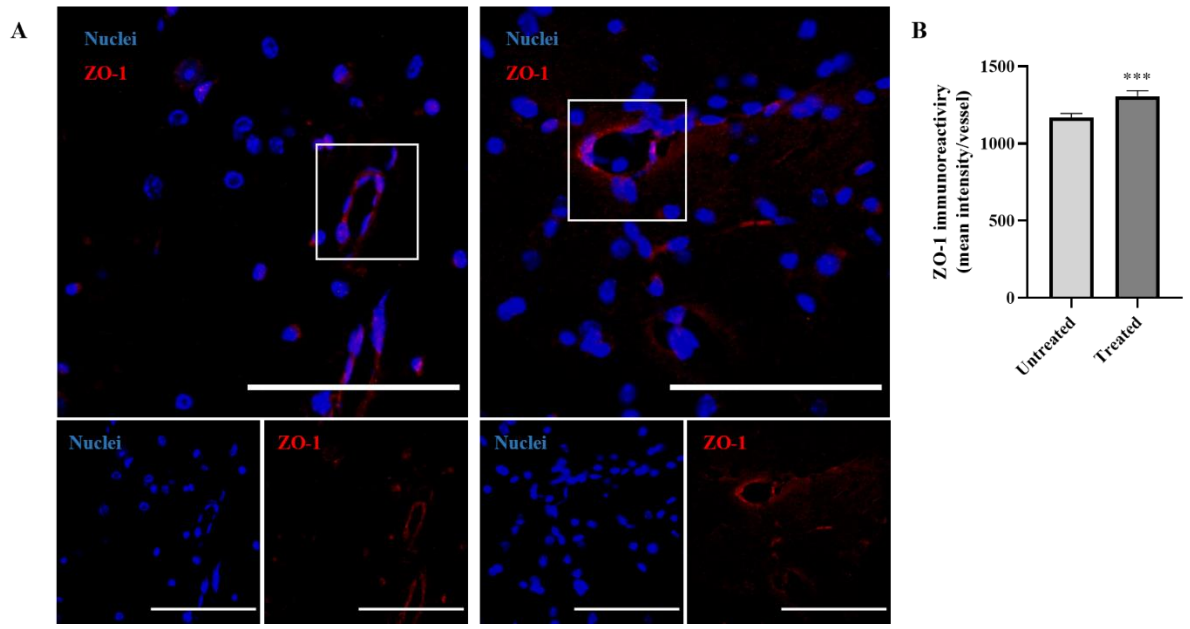

Figure 10 | Effect of RI7-MH-Lip on blood-brain barrier (BBB) properties. Triple-negative (TN) breast cancer cells (BCCs) were injected in the common carotid artery of 8-to-10-weeks-old female Balb/c mice and immunofluorescence analysis was performed in the cranial hippocampus section 10 days after. The immunofluorescence analysis of zonula occludens 1 (ZO-1, red) (**A**) revealed an increase of its immunoreactivity in the vessels (white squares) (**B**), suggesting an improvement of vessels junctional complexes and BBB properties. Hoechst 33342 was used as counterstaining for nuclei (blue). Scale bar: 100 µm. The results are expressed as mean ± SEM (n=7-8). Statistical significances were evaluated with the Kruskal-Wallis test for mean intensity. Statistical significances are denoted as *** $p<0.001$ vs untreated.

4. Effect of Ri7-MH-Lip treatment on the survival of BCBM-bearing mice

Intending to assess if Ri7-MH-Lip treatment is able to prolong survival in tumour-bearing animals, 8-to-10-weeks-old female Balb/c mice were inoculated with 4T1 cells in the common carotid artery to induce BM formation. An untreated group (n = 7) received a saline solution (NaCl 0.9%) by intravenous injection in the tail, whereas a treated group (n = 7) received liposomal injections containing equivalently 3.5 mg/Kg of MH per injection, in a total of 11 administrations in both groups. The fraction of surviving mice was monitored over time and survival time was evaluated through the Kaplan-Meier estimate[67] (Figure 11). Through a Kaplan-Meier curve, it was possible to observe that animals treated with Ri7-MH-Lip presented a prolonged survival time in comparison to the untreated group (Figure 11A).

To further support the efficacy of the treatment in prolonging the survival of tumour-bearing mice, HE staining was performed in cranial hippocampus sections (Figure 11B) and in the lungs (Supplementary figure 1) to study the pattern of BCBM formation in both groups. The histological analysis revealed fully developed metastases in the cranial hippocampus sections at 14 days post-tumour cells injection in the untreated group, by comparison to the treated one.

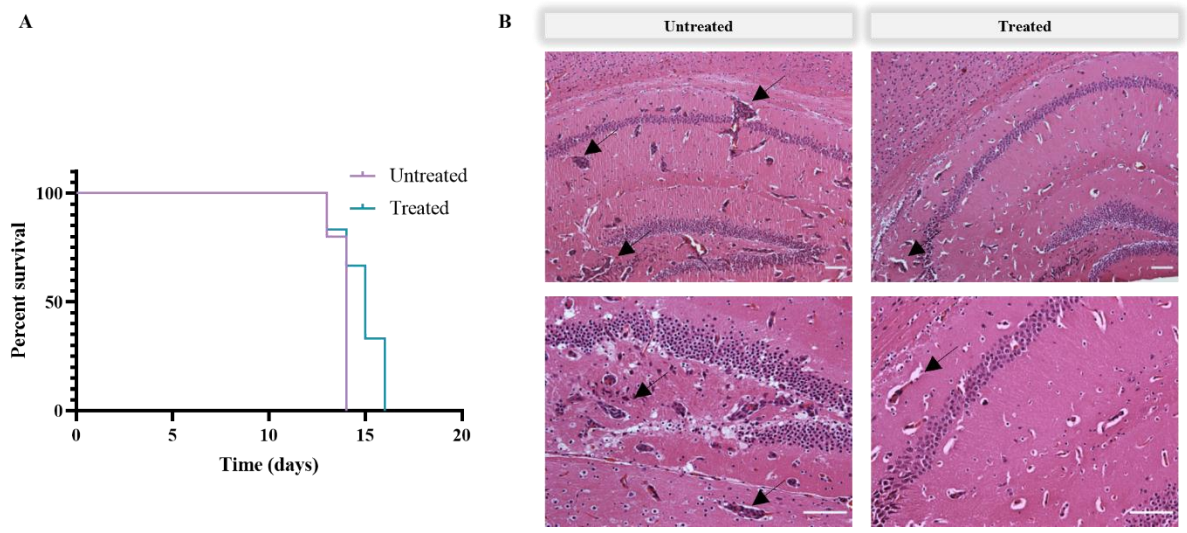

Figure 11 | Effect of Ri7-MH-Lip treatment on the survival of tumour-bearing mice. To assess the Ri7-MH-Lip effect on the survival of tumour-bearing animals, triple-negative (TN) breast cancer cells (BCCs) were injected in the common carotid artery of 8-to-10-weeks-old female Balb/c mice. A treated group received Ri7-MH-loaded liposomes (n = 7) and an untreated one received a saline solution (NaCl 0.9%, n = 7). Mice survival representation through a Kaplan-Meier curve revealed that animals treated with Ri7-MH-Lip presented a prolonged survival time in comparison to the untreated group (**A**). The pattern of BCBM colonization assessed by hematoxylin-eosin (HE) staining revealed a higher extension of metastases in cranial hippocampus sections at 14 days post-tumour cells injection in the untreated group than in the treated group (**B**). Scale bar: 100 μm.

Chapter IV - Discussion

As the leading global cancer occurrence[3], BC raises a major concern, especially in the disease's metastatic stage. The CNS is a common site for BC metastasis and, with the brain being one of the top organs in which BC most metastasizes, leaves patients with an unfortunate prognosis[1]. Despite the currently available treatments, the development of metastatic BC remains an intricate and complex disease. It represents a serious oncologic problem that has been under-investigated, despite its high incidence and shorter survival rate where only the minority of patients survive longer than 1 year[68,69].

Because there is a lack of effective treatment options for established metastases, this work brings to light an innovative strategy to affront BCBM with a preventive approach. After identifying MH as the best candidate to modulate BBB's properties and prevent BCCs adhesion in a previous study done in our laboratory[38], we developed Ri7-MH-Lip as a Trojan horse drug delivery system for a targeted delivery of the drug to the BBB's endothelial cells. The nanoformulation was tested *in vitro* and proven to be effective in improving barrier properties when in contact with metastatic cells, as well as in preventing BCCs adhesion (either to the BBB endothelium or the culture plate) (Rafaela Silvestre, Master thesis, Faculdade de Farmácia, Universidade de Lisboa, 2022; Godinho-Pereira, PhD thesis, Faculdade de Farmácia, Universidade de Lisboa, ongoing).

In vitro models are less suitable to study mechanisms related to the brain environment as they are incapable of recapitulating the bypass of metastatic cells through the BBB and escape from the brain's intrinsic immune defensive mechanisms[70]. For this reason, the present work aimed to further assess the efficacy and safety of the developed nanoformulation in a reliable BCBM animal model, as a proof-of-concept. The progress of targeted therapies against metastatic diseases has been hampered by a deficit of appropriate animal tumour models, namely of BCBM recapitulating the interactions between BCCs and BBB's endothelial cells, rendering necessary the development of a proper and faithful *in vivo* model. The most used *in vivo* metastatic models rely on tail vein injection to deliver tumour cells, facilitating the lodging of cells in the lungs, as they are the first encountered organ with a considerable capillary bed. This leads to death by large numbers of lung metastases before the BM are developed in these models[71]. Alternative injection routes primarily targeting the CNS, such as direct intracerebral and intracardiac injection, arose to induce experimental BM. However, these strategies can compromise BBB's integrity and lead to traumatic lesions. In contrast to other experimental BM animal models whose growth and progression do not parallel human BC, intracarotid artery injection of murine mammary carcinoma 4T1 cell line presents a higher reproducibility while

avoiding injection-induced CNS inflammation. It is an aggressive, highly tumorigenic and invasive TN tumour model that spontaneously metastasizes in a pattern that is analogous to human mammary cancer[72,73] while producing a smaller variation of experimental results[71]. Being previously applied in other studies[10,65,66], this model requires exceptionally microsurgical skills to successfully direct BCCs to the brain, particularly the hippocampus, rendering a suitable strategy to study BCBM[65]. The use of the intracarotid injection model enables the recapitulation of the later steps of the metastatic cascade[71], providing a unique platform to study the BCCs' migration through the BBB endothelium, which is the focus of this work. Therefore, attempts to implement this model in Portugal were put in place.

In the process of establishing a BCBM model relying on the intracarotid injection of BCCs to achieve the formation of BM in our facilities, we faced a high rate of mice's death when injecting $1x10^6$ cells in 200 µL, which was surpassed by reducing it to $0.2x10^6$ cells in 150 µL. To characterize the BCBM development in this animal model, histological analysis was performed in coronal sections of the cranial hippocampus and of the cerebellum, at different timepoints. The results obtained showed the presence of metastases at 7d as well as a gradual expansion in their number and area throughout time. On the contrary, no significant metastases were detected in the cerebellum, which is consistent with the initial model[65]. To evaluate the metastatic progress in peripheral organs, lungs, kidneys, and livers were subjected to histological analysis by HE staining. Metastases were only observed in the lungs, with an increase in tumour area throughout time, in line with previous descriptions[65].

To further characterize this BCBM mouse model, we evaluated the proliferation profile of BCCs upon colonization by assessing the expression of the proliferation marker Ki-67 by IF analysis. A significant increase in Ki-67 expression was observed during BCBM establishment and progression, showcasing a progressive proliferative phenotype of BCCs with the increase of metastatic area over time. These results are aligned with the previous notion that high levels of Ki-67 expression in BC strongly correlate with more tenacious proliferation, disease severity and, consequently, poor prognosis[10,11,74]. Together with Ki-67, Pancyt, an epithelial marker expressed by malignant cells was evaluated and shown to significantly increase with the metastatic stage of the tumour, being concomitant with previously obtained results in our laboratory[10,65]. These results advocate for the notion that, upon BCBM development, malignant cells go through MET and reacquire epithelial features, which appear essential for successful colonization of the brain parenchyma[1], as reported in our previous observations[10]. This is reinforced by the expression pattern of the epithelial marker T-lectin in established BCBM

throughout time, also in line with our previous studies[10]. The overall results illustrate an upregulation and regain of epithelial markers in BCCs, allowing them to adapt and proliferate in the brain microenvironment during BCBM formation, concurrent with the occurrence of MET[1].

As previously mentioned, several setbacks arose during the implementation of this mouse model, namely the high rate of mice's death by embolism and the complications inherent to the intracarotid injection route. Due to several obstacles and delays, this study presents some limitations, such as the *in vivo* study sample size. Even though our results show significant tendencies, it would be of interest to increase the number of animals in order to improve our trust in these observations and enhance the relevance of this study.

It is known that BBB endothelium acts as a restricted filter, shielding the brain from the body's bloodstream and limiting the penetration of most cytotoxic agents. Although the BBB's integrity is weakened upon BM's development and facilitates drug entrance in the brain, BMECs' efflux pumps bring them out again so that only a few drugs reach the brain parenchyma[75]. As conventional systemic therapy has been a challenge for BCBM treatment due to the low permeability of the BBB[76], targeted preventive therapies are needed and this work aspired to target BMECs through a liposomal approach. Aiming to disclose a pharmacological modulator able to prevent BCCs extravasation by improving BBB properties to hinder BCBM formation, previous studies performed in our laboratory exposed MH as a promising BBB modulator and its inhibitory role in BCCs migration and adhesion, hinting at its possible anti brain-metastatic effect[38].

MH, that has been proven to be clinically well tolerated, as it has been used for decades to treat bacterial infections worldwide, is of particular therapeutic interest for CNS disorders[36], since it is capable of passing the BBB endothelium and is known to have a higher tissue penetration capacity than other tetracyclines[28,33]. Moreover, MH has been linked to tumour growth inhibition in human prostate and ovarian cancer[77,78], to possess anti-inflammatory properties[32,33,79], and ability to attenuate BBB disruption after intracerebral haemorrhage, oedema, ischemia and stroke[32,35-37]. Even though MH has been used safely and effectively as an antibiotic in adult humans, some studies have suggested that it might not be completely benign[80] and, for that reason, MH's liposome encapsulation arises to overcome the potential cytotoxicity associated with higher doses, reducing the required concentrations. For this reason, and to specially target BBB's endothelial cells, *in vitro* studies perfomed in our group aimed to

establish the capacity of MH-loaded liposomes in a BBB-targeting drug delivery system to prevent BCCs transmigration across BMECs (Rafaela Silvestre, Master thesis, Faculdade de Farmácia, Universidade de Lisboa, 2022; Joana Godinho-Pereira, PhD thesis, Faculdade de Farmácia, Universidade de Lisboa, ongoing). It was possible to confirm MH's safety profile in the barrier endothelium and to validate this drug's potential as a preventive treatment for BCBM. Taking these results into account, it was postulated that MH might be successful in modulating barrier properties preventing of BCCs transmigration and BCBM development *in vivo*.

There are numerous advantages to using liposomes as a drug delivery system, such as the protection against the biological microenvironment. However, in the present work, liposomes were used to enhance the cellular delivery of MH to the BBB's endothelium using TfRAb as trojan horse targeting moiety, allowing BMECs' targeting and the use of non-cytotoxic levels of MH. The vast majority of studies employing liposomal approaches targeting the BBB aims at surpassing it and reaching the brain, however, this work focused on reaching the BBB endothelium and act upon BMECs. Previous *in vivo* studies exploited Ri7-functionalized liposomes demonstrating a higher uptake in the brain endothelium when compared to non-functionalized ones[53] and once associated to the luminal side of BMECs, they are very likely to be taken up by the endothelium[64], thus motivating the choice of this ligand to efficiently target the BBB endothelium.

A fundamental step of preclinical studies for new drugs is safety assessment, which is directly related to the drug's approval. BMECs' viability evaluation upon Ri7-MH-loaded liposomes treatment was formerly assessed to dismiss toxic concentrations and narrow treatment timepoints. This study validated the safe use of MH in BBB endothelium (Rafaela Silvestre, Master thesis, Faculdade de Farmácia, Universidade de Lisboa, 2022; Joana Godinho-Pereira, PhD thesis, Faculdade de Farmácia, Universidade de Lisboa, ongoing). Additionally, a summary of systemic exposure data in toxicology studies concluded that 50 mg/Kg/day was the maximum dose of free MH at which no substantial toxicity was observed in mice[81]. In this work, we chose to use a concentration of equivalently 3.5 mg of MH per Kg of animal encapsulated into Ri7-functionalized liposomes due to the liposomes' loading capacity, which is within a secure range according to the FDA approved dose.

Following this previous *in vitro* work, *in vivo* studies were conducted to ascertain the safety of Ri7-MH-loaded liposomes' treatment on general mouse health, based on body weight as well

as on blood parameters analysis of mice. When comparing the mice group receiving the liposomal formulation with the untreated one, it was possible to observe a similar body weight since the first injection, and no severe alterations in mice's general health, evidencing the safety of the treatment.

As suggested by WHO[82] and other animal research guidelines[83,84], to ascertain if the treatment presents any toxic effects to the mice, toxicity indicators of hepatic, renal and cardiac toxicity were evaluated along with histological analysis of hearts, lungs, livers, kidneys and brains. Since the liver and kidneys are usually responsible for metabolism and excretion, potential toxic agents can easily affect them. The histological analysis revealed no signs of deterioration in the treated mice. Regarding the serum analysis, there were no significant differences between the biochemical parameters of control and MH-treated mice. The overall results indicate that the Ri7-MH-Lip treatment does not present any type of peripheral toxicity, supporting the safety of this preventive approach.

The potential of Ri7-MH-Lip treatment in preventing BCCs' transmigration was based on the BM's presence analysis between the untreated vs treated groups where both metastases number and area were evaluated. Upon this experiment, it was possible to observe substantial prevention in BCBM formation upon Ri7-MH-loaded liposomes' intravenous injection. Metastases number was shown to be decreased when the mice were treated with Ri7-MH-Lip, as opposed to the tumour's area that suffered no significant alterations. These differences might be a result of fewer BCCs extravasating through the BBB causing a lower number of individual tumours in which these cells maintain their proliferative capacity and ability to colonize the brain parenchyma.

It is believed that the development of BM depends on the unique interaction between BCCs and BMECs and this interplay plays an important role in BCBM formation[18]. Being the foremost controllers of paracellular permeability, TJs are compromised during the interaction between BCCs and BMECs[85], serving as a major physiological determinant in BBB's function. The disruption of junctional complexes has been reported in the context of BM formation, leading to an increase in brain permeation, a phenomenon that has also been associated with BCCs' paracellular transmigration[10,86]. With this in mind, this work aimed to instigate BBB's properties and assess MH treatment's potential in preventing BCCs' extravasation into the brain. To this end, ZO-1, a protein associated with the functional integrity of TJs in cerebral endothelium[87], was examined. IF analysis of BMECs exposed to BCCs showcased an increment

in ZO-1 expression at the vessels upon Ri7-MH-Lip treatment, suggesting an increment in the barrier's integrity and function. Overall, these findings suggest that the interaction between metastatic cells and BMECs compromises BBB's integrity by mitigating TJs expression, thus promoting BBB's permeation. Moreover, due to the alterations observed at the endothelial level, we can endorse a previous belief that a likely paracellular mechanism is responsible for BCCs' transposition of the BBB[18].

With this work we further aimed to ascertain if the Ri7-MH-Lip treatment can, not only prevent BCCs transmigration into the brain, but also extend the life span of mice with established BCBM. In this sense, the survival time of treated and untreated groups was examined through a Kaplan-Meier estimate[67] and a higher survival time was observed in the treated one. Metastases presence was further confirmed by histological analysis in cranial hippocampus sections where it was possible to observe a substantial reduction in established BCBM in treated mice. These results suggest that the treatment was successful in extending the survival time of BCBM-bearing mice and validated the intrinsic protection provided by the Ri7-MH-Lip throughout mice's lifespan.

It is known that the life expectancy of humans rounds 80 years, while the average lifespan of laboratory mice is about 24 months and sexual maturity is attained within an average of 10 weeks. The biological age reflects the development rate which changes in the different periods of life and is useful to distinguish between the several stages of growth[88]. Tumour susceptibility depends more on the biological age than on the chronologic one[89]. Correlation studies based on the strength of lifespan and growth stages suggest that 1 day in adult mice can reach the equivalent of 30 days to a year in humans, which supports our hypothesis that the treatment might be able to increase the average life expectancy in humans bearing BCBM.

Taken together, these results highly support the potential of Ri7-MH-Lip treatment as a safe and efficient approach to hinder BC's metastatic consequences through the preservation of BBB's cohesion and prevention of BCBM formation.

Chapter V - Conclusion and future perspectives

Even though relevant improvements in patient's survival have been made regarding early diagnosis of BC, metastatic disease is still incurable with the currently available therapies. BM arise as an urgent unmet medical need due to the restricted permeability of the BBB, averting the passage of most therapeutic agents. With this in mind, this work emerges as an innovative approach to confront BCBM development *in vivo* by focusing on the prevention, rather than tackling the established devastating disease. With our work, it was possible to implement and characterize a reliable animal model of BCBM, essential to ascertain the potential of therapeutic strategies directed to such pathology. Moreover, it was demonstrated the efficacy of a recently developed nanoformulation to specifically deliver MH to the BBB endothelium and prevent BCCs transmigration and consequent formation of BCBM, while preserving the integrity of the BBB *in vivo*. Importantly, the safety of Ri7-MH-Lip treatment was demonstrated alongside with its ability to prolong the survival of BCBM-bearing mice.

The next step to take in the future would be to minutely characterize the treatment's effect on BBB's behaviour at different stages after BCCs inoculation through the analysis of other junctional proteins, such as β-catenin, along with the analysis of TJs ZO-1 and MMP-9 interplay at a less advanced stage of BM development. Finally, it would be of interest to inquire about the effect of Ri7-MH-Lip in adhesion molecules, such as E-selectin, which are exclusively expressed in BMECs upon BCCs invasion.

To conclude, the present thesis was able to provide the proof-of-concept of MH's neuroprotective properties in the BBB endothelium against BCCs-induced disruption. This approach arises as a scientific advance in the development of a new preventive therapy for BCBM, representing an advance beyond the current state-of-the-art in Neurooncology. Remarkably, it paves the way for MH repurposing for BCBM prevention, shortening the path for the implementation of a preventive pharmacologic strategy for BC patients.

Chapter VI - Supplementary Material

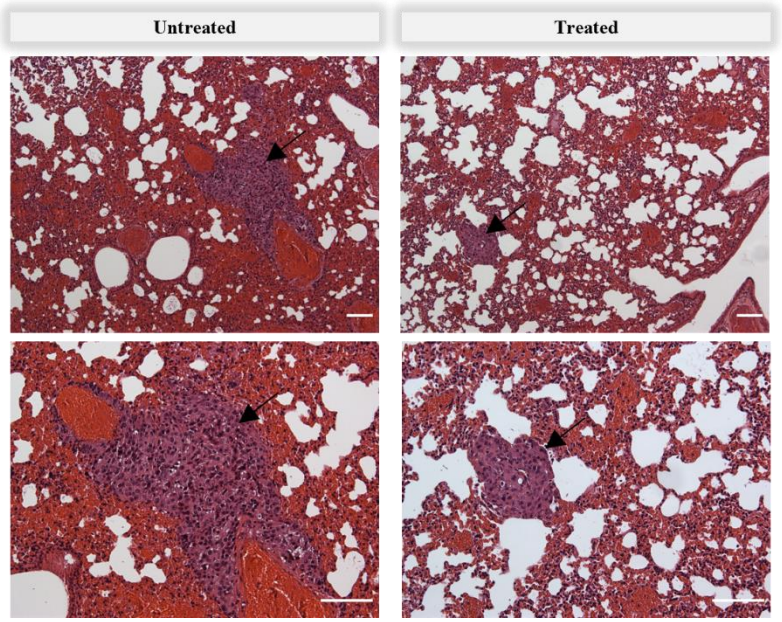

Supplementary figure 1 | Lungs histological analysis of Ri7-MH-Lip-treated mice. To assess the Ri7-MH-Lip effect on the survival of tumour-bearing animals, triple-negative (TN) breast cancer cells (BCCs) were injected in the common carotid artery of 8-to-10-weeks-old female Balb/c mice. A treated group of mice (n = 7) received Ri7-MH-loaded liposomes, whereas an untreated group (n = 7) received a saline solution (NaCl 0.9%). The histological analysis by hematoxylin-eosin staining revealed metastases (black arrows) in the lungs after BCCs cells injection in the control group (untreated) by comparison to the treated group. Scale bar: 100 µm.

Chapter VII - References

1. Custódio-Santos T, Videira M, Brito MA. Brain metastasization of breast cancer. *Biochim Biophys Acta Rev Cancer*. 2017;1868(1):132-147. doi:10.1016/j.bbcan.2017.03.004

2. Thomas M, Kelly ED, Abraham J, Kruse M. Invasive lobular breast cancer: A review of pathogenesis, diagnosis, management, and future directions of early stage disease. *Semin Oncol*. Apr 2019;46(2):121-132. doi:10.1053/j.seminoncol.2019.03.002

3. Hyuna S, Jacques F, Rebecca LS, et al. Global Cancer Statistics 2020: GLOBOCAN Estimates of Incidence and Mortality Worldwide for 36 Cancers in 185 Countries. *CA Cancer J Clin*. 2021;71(3):209–249. doi:10.3322/caac.21660.

4. Tao ZQ, Shi A, Lu C, Song T, Zhang Z, Zhao J. Breast Cancer: Epidemiology and Etiology. *Cell Biochem Biophys*. 2015;72(2):333-338. doi:10.1007/s12013-014-0459-6

5. Ni W, Chen W, Lu Y. Emerging findings into molecular mechanism of brain metastasis. *Cancer Med*. Aug 2018;7(8):3820-3833. doi:10.1002/cam4.1667

6. Bryan S, Witzel I, Borgmann K, Oliveira-ferrer L. Molecular Mechanisms Associated with Brain Metastases in HER2-Positive and Triple Negative Breast Cancers. *Cancers (Basel)*. 2021;13(16):4137. doi:10.3390/cancers13164137.

7. Lowery FJ, Yu D. Brain metastasis: Unique challenges and open opportunities. *Biochim Biophys Acta Rev Cancer*. 2017;1867(1):49-57. doi:10.1016/j.bbcan.2016.12.001

8. Fak II, Signaling E, Shen M, et al. Tinagl1 Suppresses Triple-Negative Breast Cancer Progression and Metastasis by Simultaneously Inhibiting Integrin/FAK and EGFR Signaling. *Cancer Cell*. 2019;35(1):64-80.e7. doi:10.1016/j.ccell.2018.11.016

9. Adrienne G. Waks MEPW, MD. Breast Cancer Treatment A Review. *JAMA*. 2019;321(3):288-300. doi:10.1001/jama.2018.19323

10. Figueira I, Galego S, Custódio-Santos T, et al. Picturing Breast Cancer Brain Metastasis Development to Unravel Molecular Players and Cellular Crosstalk. *Cancers (Basel)*. 2021;13(4):910. doi:10.3390/cancers13040910

11. Galego S, Kauppila LA, Malhó R, Pimentel J, Brito MA. Myocyte Enhancer Factor 2C as a New Player in Human Breast Cancer Brain Metastases. *Cells*. 2021;10(2):378. doi:10.3390/cells10020378

12. Wang Y, Ye F, Liang Y, Yang Q. Breast cancer brain metastasis: insight into molecular mechanisms and therapeutic strategies. *Br J Cancer*. 2021;125(8):1056-1067. doi:10.1038/s41416-021-01424-8

13. Neophytou C, Boutsikos P, Papageorgis P. Molecular mechanisms and emerging therapeutic targets of triple-negative breast cancer metastasis. *Frontiers in Oncology*. 2018;8(31)doi:10.3389/fonc.2018.00031

14. Strell C, Entschladen F. Extravasation of leukocytes in comparison to tumor cells. *Cell Commun Signal*. 2008;6:10. doi:10.1186/1478-811X-6-10

15. Läubli H, Borsig L. Selectins promote tumor metastasis. *Semin Cancer Biol*. 2010;20(3):169-177. doi:10.1016/j.semcancer.2010.04.005

16. Blecharz KG, Colla R, Rohde V, Vajkoczy P. Control of the blood-brain barrier function in cancer cell metastasis. *Biol Cell*. 2015;107:342-371. doi:10.1111/boc.201500011

17. Brayton J, Qing Z, Hart MN, Vangilder JC, Fabry Z. Influence of adhesion molecule expression by human brain microvessel endothelium on cancer cell adhesion. *J Neuroimmunol*. 1998;89(1-2):104-112. doi:10.1016/s0165-5728(98)00127-1

18. Herman H, Fazakas C, Haskó J, et al. Paracellular and transcellular migration of metastatic cells through the cerebral endothelium. *J Cell Mol Med*. 2019;23(4):2619-2631. doi:10.1111/jcmm.14156

19. Reymond N, d'Agua BB, Ridley AJ. Crossing the endothelial barrier during metastasis. *Nat Rev Cancer*. Dec 2013;13(12):858-70. doi:10.1038/nrc3628

20. Lundy DJ, Nguy H, Hsieh PCH. Emerging Nano-Carrier Strategies for Brain Tumor Drug Delivery and Considerations for Clinical Translation. *Pharmaceutics*. 2021;13(8):1193. doi:10.3390/pharmaceutics13081193

21. Wilhelm I, Molnár J, Fazakas C, Haskó J, Krizbai IA. Role of the blood-brain barrier in the formation of brain metastases. *Int J Mol Sci*. 2013;14(1):1383-1411. doi:10.3390/ijms14011383

22. Zhao Z, Nelson AR, Betsholtz C, Zlokovic BV, Angeles L. Establishment and dysfunction of the BBB. *Cell*. 2015;163(5):1064-1078. doi:10.1016/j.cell.2015.10.067

23. Moura RP, Cláudia Martins, Soraia Pinto, Flávia Sousa, Bruno, Sarmento. Blood-brain barrier receptors and transporters: an insight on their function and how to exploit them through nanotechnology. *Expert Opin Drug Deliv*. 2019;16(3):271-285. doi:10.1080/17425247.2019.1583205

24. Cardoso F, Brites D, Brito M. Looking at the blood–brain barrier: Molecular anatomy and possible investigation approaches. *Brain Res Rev*. 2010;64(2):328-363. doi:10.1016/j.brainresrev.2010.05.003

25. Sharif Y, Jumah F, Coplan L, Krosser A, Sharif K, Tubbs RS. Blood brain barrier: A review of its anatomy and physiology in health and disease. *Clin Anat*. 2018;31(1):812-823. doi:10.1002/ca.23083

26. Bauer H-C, Krizbai IA, Bauer H, Traweger A. "You Shall Not Pass"-tight junctions of the blood brain barrier. *Front Neurosci*. 2014;8:392. doi:10.3389/fnins.2014.00392

27. Bellettato CM, Scarpa M. Possible strategies to cross the blood-brain barrier. *Ital J Pediatr*. Nov 16 2018;44(Suppl 2):131. doi:10.1186/s13052-018-0563-0

28. Garrido-Mesa N, Zarzuelo A, Gálvez J. Minocycline: far beyond an antibiotic. *Br J Pharmacology*. 2013;169(2):337-352. doi:10.1111/bph.12139

29. Yang L, Sugama S, Chirichigno JW, et al. Minocycline Enhances MPTP Toxicity to Dopaminergic Neurons. *J Neurosci Res*. 2003;285:278-285. doi:10.1002/jnr.10709

30. Good ML, Hussey DL. Minocycline: Stain devil? *Br J Dermatology*. 2003;149(2):237-239. doi:10.1046/j.1365-2133.2003.05497.x

31. Saivin S, Houin G. Clinical Pharmacokinetics of Doxycycline and Minocycline. *Clin Pharmacokinet*. 1988;15(6):355-366. doi:10.2165/00003088-198815060-00001

32. Yrjänheikki J, Tikka T, Keinänen R, Goldsteins G, Chan PH, Koistinaho J. A tetracycline derivative, minocycline, reduces inflammation and protects against focal cerebral ischemia with a wide therapeutic window. *Proc Natl Acad Sci U S A*. 1999;96(23):13496-13500. doi:10.1073/pnas.96.23.13496

33. Yong VW, Wells J, Giuliani F, Casha S, Power C, Metz LM. The promise of minocycline in neurology. *Lancet Neurol*. 2004;3(12):744-751. doi:10.1016/S1474-4422(04)00937-8

34. Tomás-Camardiel M, Rite I, Herrera AJ, et al. Minocycline reduces the lipopolysaccharide-induced inflammatory reaction, peroxynitrite-mediated nitration of proteins, disruption of the blood-brain barrier, and damage in the nigral dopaminergic system. *Neurobiol Dis*. 2004;16:190-201. doi:10.1016/j.nbd.2004.01.010

35. Yang Y, Salayandia VM, Thompson JF, Yang LY, Estrada EY, Yang Y. Attenuation of acute stroke injury in rat brain by minocycline promotes blood–brain barrier remodeling and alternative microglia/macrophage activation during recovery. *J Neuroinflammation*. 2015;12:26. doi:10.1186/s12974-015-0245-4

36. Wasserman JK, Schlichter LC. Minocycline protects the blood–brain barrier and reduces edema following intracerebral hemorrhage in the rat. *Exp Neurol*. 2007;207:227-237. doi:10.1016/j.expneurol.2007.06.025

37. Wang G, Li Z, Li S, et al. Minocycline Preserves the Integrity and Permeability of BBB by Altering the Activity of DKK1–Wnt Signaling in ICH Model. *Neuroscience*. 2019;415:135-146. doi:10.1016/j.neuroscience.2019.06.038

38. Godinho-Pereira J, Lopes MD, Garcia AR, et al. A Drug Screening Reveals Minocycline Hydrochloride as a Therapeutic Option to Prevent Breast Cancer Cells Extravasation across the Blood-Brain Barrier. *Biomedicines*. 2022;10(8):1988. doi:10.3390/biomedicines10081988

39. Juhairiyah F, de Lange ECM. Understanding Drug Delivery to the Brain Using Liposome-Based Strategies: Studies that Provide Mechanistic Insights Are Essential. *AAPS J*. 2021;23(6):114. doi:10.1208/s12248-021-00648-z

40. Agrawal M, Tripathi DK, Saraf S, et al. Recent advancements in liposomes targeting strategies to cross blood-brain barrier (BBB) for the treatment of Alzheimer ' s disease. *J Control Release*. 2017;260:61-77. doi:10.1016/j.jconrel.2017.05.019

41. Pinheiro RGR, Coutinho AJ, Pinheiro M, Neves AR. Nanoparticles for Targeted Brain Drug Delivery: What Do We Know? *Int J Mol Sci*. 2021;22(21):11654. doi:10.3390/ijms222111654

42. Patel MM, Patel BM. Crossing the Blood–Brain Barrier: Recent Advances in Drug Delivery to the Brain. *CNS Drugs*. 2017;31(2):109-133. doi:10.1007/s40263-016-0405-9

43. Song J, Lu C, Leszek J, Zhang J. Design and development of nanomaterial-based drug carriers to overcome the blood–brain barrier by using different transport mechanisms. *Int J Mol Sci*. 2021;22(18):10118. doi:10.3390/ijms221810118

44. Markoutsa E, Pampalakis G, Niarakis A, et al. Uptake and permeability studies of BBB-targeting immunoliposomes using the hCMEC / D3 cell line. *Eur J Pharm and Biopharm*. 2011;77(2):265-274. doi:10.1016/j.ejpb.2010.11.015

45. Huwyler J, Wu D, Pardridge WM. Brain drug delivery of small molecules using immunoliposomes. *Proc Natl Acad Sci U S A*. 1996;93(24):14164-14169. doi:10.1073/pnas.93.24.14164

46. Hu W, Metselaar J, Ben L-H, et al. PEG Minocycline-Liposomes Ameliorate CNS Autoimmune Disease. *PLoS One*. 2009;4(1):e4151. doi:10.1371/journal.pone.0004151

47. Pathan S, Iqbal Z, Zaidi S, et al. CNS Drug Delivery Systems: Novel Approaches. *Recent Pat Drug Deliv Formul*. 2009;3(1):71-89. doi:10.2174/187221109787158355

48. Boado RJ, Pardridge WM. The Trojan Horse Liposome Technology for Nonviral Gene Transfer across the Blood-Brain Barrier. *J Drug Deliv*. 2011;2011:296151. doi:10.1155/2011/296151

49. Pardridge WM. Brain Delivery of Nanomedicines : Trojan Horse Liposomes for Plasmid DNA Gene Therapy of the Brain. *Front Med Technol*. 2020;2:602236. doi:10.3389/fmedt.2020.602236

50. Sanchez-Covarrubias L, Slosky L, Thompson B, Davis T, Ronaldson P. Transporters at CNS Barrier Sites: Obstacles or Opportunities for Drug Delivery? *Curr Pharm Des*. 2014;20(10):1422-1449. doi:10.2174/13816128113199990463

51. Johnsen KB, Burkhart A, Thomsen LB, Andresen TL, Moos T. Targeting the transferrin receptor for brain drug delivery. *Prog Neurobiol*. 2019;181:101665. doi:10.1016/j.pneurobio.2019.101665

52. Fishman JB, Rubin JB, Handrahan JV, Connor JR, Fine RE. Receptor-mediated transcytosis of transferrin across the blood-brain barrier. *J Neurosci Res*. 1987;18(2):299-304. doi:10.1002/jnr.490180206

53. Rooy IV, Mastrobattista E, Storm G, Hennink WE, Schiffelers RM. Comparison of five different targeting ligands to enhance accumulation of liposomes into the brain. *J Control Release*. 2011;150(1):30-36. doi:10.1016/j.jconrel.2010.11.014

54. Sehlin D, Syvänen S. Engineered antibodies: new possibilities for brain PET? *Eur J Nucl Med Mol Imaging*. 2019;46(13):2848-2858. doi:10.1007/s00259-019-04426-0

55. Rip J. Liposome technologies and drug delivery to the CNS. *Drug Disc Today: Technol*. 2016;20:53-58. doi:10.1016/j.ddtec.2016.07.005

56. Pardridge WM. Delivery of Biologics Across the Blood-Brain Barrier with Molecular Trojan Horse Technology. *BioDrugs*. 2017;31(6):503-519. doi:10.1007/s40259-017-0248-z

57. Kang S, Duan W, Zhang S, Chen D, Feng J, Qi N. Muscone/RI7217 co-modified upward messenger DTX liposomes enhanced permeability of blood – brain barrier and targeting glioma. *Theranostics*. 2020;10(10):4308-4322. doi:10.7150/thno.41322

58. Pardridge WM. Blood-brain barrier drug delivery of IgG fusion proteins with a transferrin receptor monoclonal antibody. *Expert Opin Drug Deliv*. 2015;12(2):207-222. doi:10.1517/17425247.2014.952627

59. Paris-robidas S, Emond V, Tremblay C, Soulet D. In Vivo Labeling of Brain Capillary Endothelial Cells after Intravenous Injection of Monoclonal Antibodies Targeting the Transferrin Receptor. *Mol Pharmacol*. 2011;80(1):32-39. doi:10.1124/mol.111.071027

60. Lee HJ, Engelhardt B, Lesley J, Bickel U, Pardridge WM. Targeting rat anti-mouse transferrin receptor monoclonal antibodies through blood-brain barrier in mouse. *J Pharmacol Exp Ther*. 2000;292:1048-1052.

61. Paris-robidas S, Brouard D, Emond V. Internalization of targeted quantum dots by brain capillary endothelial cells in vivo. *J Cereb Blood Flow Metab*. 2016;36(4):731-742. doi:10.1177/0271678X15608201

62. Bendix K, Bak M, Melander F, et al. Modulating the antibody density changes the uptake and transport at the blood-brain barrier of both transferrin receptor-targeted gold nanoparticles and liposomal cargo. *J Control Release*. 2019;295:237-249. doi:10.1016/j.jconrel.2019.01.005

63. Bouchoucha M, Béliveau É, Kleitz F, Calon F, Fortin M-A. Antibody-conjugated mesoporous silica nanoparticles for brain microvessel endothelial cell targeting. *J Mater Chem B*. 2017;5(37):7721-7735. doi:10.1039/c7tb01385j

64. Kucharz K, Kristensen K, Johnsen KB, et al. Post-capillary venules are the key locus for transcytosis-mediated brain delivery of therapeutic nanoparticles. *Nat Commun*. Jul 5 2021;12(1):4121. doi:10.1038/s41467-021-24323-1

65. Sereno M, Haskó J, Molnár K, et al. Downregulation of circulating miR 802-5p and miR 194-5p and upregulation of brain MEF2C along breast cancer brain metastasization. *Mol Oncol*. 2020;14(3):520-538. doi:10.1002/1878-0261.12632

66. Zhang C, Lowery FJ, Yu D. Intracarotid Cancer Cell Injection to Produce Mouse Models of Brain Metastasis. *J Vis Exp*. 2017;(120):55085. doi:10.3791/55085

67. Goel MK, Khanna P, Kishore J. Understanding survival analysis: Kaplan-Meier estimate. *Int J Ayurveda Res*. Oct 2010;1(4):274-8. doi:10.4103/0974-7788.76794

68. Laakmann E, Witzel I, Fasching PA, et al. Development of central nervous system metastases as a first site of metastatic disease in breast cancer patients treated in the neoadjuvant trials GeparQuinto and GeparSixto. *Breast Cancer Res*. May 10 2019;21(1):60. doi:10.1186/s13058-019-1144-x

69. Jin J, Gao Y, Zhang J, et al. Incidence, pattern and prognosis of brain metastases in patients with metastatic triple negative breast cancer. *BMC Cancer*. Apr 19 2018;18(1):446. doi:10.1186/s12885-018-4371-0

70. Hasko J, Fazakas C, Molnar K, et al. Response of the neurovascular unit to brain metastatic breast cancer cells. *Acta Neuropathol Commun*. Aug 19 2019;7(1):133. doi:10.1186/s40478-019-0788-1

71. Zhang C, Yu D. Microenvironment determinants of brain metastasis. *Cell Biosci*. Feb 25 2011;1(1):8. doi:10.1186/2045-3701-1-8

72. Tao K, Fang M, Alroy J, Sahagian GG. Imagable 4T1 model for the study of late stage breast cancer. *BMC Cancer*. Aug 9 2008;8:228. doi:10.1186/1471-2407-8-228

73. Pulaski BA, Ostrand-Rosenberg S. Mouse 4T1 breast tumor model. *Curr Protoc Immunol*. 2001;20:Unit 20 2. doi:10.1002/0471142735.im2002s39

74. Zhu X, Chen L, Huang B, et al. The prognostic and predictive potential of Ki-67 in triple-negative breast cancer. *Sci Rep*. Jan 14 2020;10(1):225. doi:10.1038/s41598-019-57094-3

75. Kim JS, Kim IA. Evolving treatment strategies of brain metastases from breast cancer: current status and future direction. *Ther Adv Med Oncol*. 2020;12:1-21. doi:10.1177/1758835920936117

76. Bailleux C, Eberst L, Bachelot T. Treatment strategies for breast cancer brain metastases. *Br J Cancer*. 2021;124(1):142–155. doi:10.1038/s41416-020-01175-y

77. Regen F, Heuser I, Herzog I, Hellmann-Regen J. Striking growth-inhibitory effects of minocycline on human prostate cancer cell lines. *Urology*. Feb 2014;83(2):509 e1-6. doi:10.1016/j.urology.2013.10.029

78. Pourgholami MH, Mekkawy AH, Badar S, Morris DL. Minocycline inhibits growth of epithelial ovarian cancer. *Gynecol Oncol*. May 2012;125(2):433-40. doi:10.1016/j.ygyno.2012.01.006

79. Stirling DP, Koochesfahani KM, Steeves JD, Tetzlaff W. Minocycline as a Neuroprotective Agent. *Neuroscientist*. 2005;11:308-322. doi:10.1177/1073858405275175

80. Xing C, Levchenko T, Guo S, Stins M, Torchilin VP, Lo EH. Delivering minocycline into brain endothelial cells with liposome-based technology. *J Cereb Blood Flow Metab*. 2012;32(6):983-988. doi:10.1038/jcbfm.2012.48

81. See NA. Pharmacology/Toxicology review and evaluation. *FDA*. 2006;(50-808)

82. Organization WH. General guidelines for methodologies on research and evaluation of traditional medicine. 2000;(WHO/EDM/TRM/2000.1)

83. Nigatu TA, Afework M, Urga K, Ergete W, Makonnen E. Toxicological investigation of acute and chronic treatment with Gnidia stenophylla Gilg root extract on some blood parameters and histopathology of spleen, liver and kidney in mice. *BMC Res Notes*. 2017;10(1):625. doi:10.1186/s13104-017-2964-3

84. Kilkenny C, Browne WJ, Cuthill IC, Emerson M, Altman DG. Improving bioscience research reporting: the ARRIVE guidelines for reporting animal research. *Vet Clin Pathol*. 2010;8(6):e100041. doi:10.1111/j.1939-165X.2012.00418.x

85. Zhang S, An Q, Wang T, Gao S, Zhou G. Autophagy- and MMP-2/9-mediated Reduction and Redistribution of ZO-1 Contribute to Hyperglycemia-increased Blood–Brain Barrier Permeability During Early Reperfusion in Stroke. *Neuroscience* 2018;377:126-137. doi:10.1016/j.neuroscience.2018.02.035

86. Godinho-Pereira J, Garcia AR, Figueira I, Malhó R, Brito MA. Behind Brain Metastases Formation: Cellular and Molecular Alterations and Blood–Brain Barrier Disruption. *Int J Mol Sci*. 2021; 22(13):7057. doi:10.3390/ijms22137057

87. Asahi M, Wang X, Mori T, Sumii T, Fini ME, Lo EH. Effects of Matrix Metalloproteinase-9 Gene Knock-Out on the Proteolysis of Blood–Brain Barrier and White Matter Components after Cerebral Ischemia. *J Neurosci*. 2001;21(19):7724–7732. doi:10.1523/JNEUROSCI.21-19-07724.2001

88. Dutta S, Sengupta P. Men and mice: Relating their ages. *Life Sci*. 2015;(152):244-248. doi:10.1016/j.lfs.2015.10.025

89. Wang S, Lai X, Deng Y, Song Y. Correlation between mouse age and human age in anti-tumor research: Significance and method establishment. *Life Sci*. Feb 1 2020;242:117242. doi:10.1016/j.lfs.2019.117242